UNIVERSITÀ
DEGLI STUDI
DI PADOVA

Sede Amministrativa: Università degli Studi di Padova

Dipartimento di Scienze Cardiologiche, Toraciche e Vascolari

CORSO DI DOTTORATO DI RICERCA IN:
SCIENZE MEDICHE, CLINICHE E SPERIMENTALI

CURRICOLO: METODOLOGIA CLINICA, SCIENZE ENDOCRINOLOGICHE,
DIABETOLOGICHE E NEFROLOGICHE

CICLO 29°

In vitro and in vivo study of NETosis in diabetic wound healing

Coordinatore: Ch.mo Prof. Roberto Vettor
Supervisore: Ch.mo Prof. Angelo Avogaro
Co-Supervisore: Ch.mo Prof. Gian Paolo Fadini

Dottorando: Dott.ssa Valentina Scattolini

Summary

Abstract

People with diabetes have an increased risk of developing several serious health problems. One of the most frequent complication is an impaired wound healing.

Neutrophils are recruited early to the wound bed and, upon activation, they undergo histone citrullination by protein arginine deiminase (PAD)4, exocytosis of chromatin and enzymes as neutrophil extracellular traps (NETs), and death. This process is called NETosis. In diabetes, neutrophils are primed to release NETs and die by NETosis. Although this process is a defense against infection, excessive NETosis can damage tissue.

The aim of this study was to examine the effect of NETosis on the healing of diabetic foot ulcers (DFUs). Using proteomics, we found that NET components were enriched in non-healing human DFUs. In an independent validation cohort, a high concentration of neutrophil elastase in the wound was associated with infection and a subsequent worsening of the ulcer. NET components were elevated in the blood of patients with DFUs. Neutrophils isolated from the blood of DFU patients showed an increased spontaneous NETosis, but an impaired inducible NETosis. We have set up a system of intravital microscopy to monitor the presence of neutrophils in a mouse model of ulcer; this imaging technique, in addition to FACS detection of histone citrullination, showed that (1) PAD4 activity was increased by diabetes and (2) NETosis occurred in the bed of excisional wounds.

PAD4 inhibition by Cl-amidine reduced NETting neutrophils and rescued wound healing in diabetic mice. Cumulatively, these data suggest that NETosis delays DFU healing and its modulation could be a therapeutic strategy to improve outcome of DFU in diabetic patients.

Riassunto

La FID, Federazione Internazionale del Diabete, paragona questa patologia ad una vera e propria epidemia inarrestabile. Una delle gravi complicanze causata da questa malattia sono le ulcere nel piede del diabetico (DFU, Diabetic Foot Ulcer): infatti la guarigione delle ferite è compromessa in molti pazienti diabetici e ciò provoca un aumentato rischio di morbilità e mortalità.

I neutrofili sono le principali cellule coinvolte nelle prime fasi della guarigione delle ulcere, in quanto sono la principale componente cellulare reclutata in sede di danno tissutale. I neutrofili hanno un ruolo fondamentale nel sistema immunitario innato e rappresentano la prima difesa contro l'infezione da patogeni. Questa attività antimicrobica è resa possibile anche da un tipo di morte cellulare tipico dei neutrofili al quale è stato dato il nome di NETosi. La NETosi si differenzia da necrosi, apoptosi, necroptosi e autofagia. E' innescata da PAD4 (Peptidil Arginine Deaminase 4) che è un enzima nucleare Ca^{2+}-dipendente appartenente alla superfamiglia delle amidinotransferasi, coinvolto nella citrullinazione degli istoni. A questa fase seguono la decondensazione della cromatina, la migrazione dell'elastasi all'interno del nucleo e la rottura della membrana nucleare con il conseguente rilascio di DNA sottoforma di filamenti. Questi filamenti, chiamati NETs (Neutrophil Extracellular Traps), sono composti da enzimi e proteine granulari e da materiale nucleare, il cui compito è quello di intrappolare fisicamente i patogeni e le loro componenti, fino alla lisi cellulare. Questo processo è alterato nel diabete e può provocare danni ai tessuti, causando un ritardo nella guarigione delle ferite.

Lo scopo di questo progetto è stato quello di studiare gli effetti della NETosi sulla guarigione delle ulcere dei pazienti diabetici, avvalendoci anche dell'uso di un modello sperimentale animale. L'analisi proteomica iniziale ci ha permesso di identificare le proteine coinvolte in questo processo; inoltre, abbiamo osservato che nel sangue dei pazienti diabetici vi è una sovra-espressione di alcuni di questi componenti. I neutrofili isolati da questi pazienti mostrano:

1- un incremento della NETosi spontanea;
2- un'alterata NETosi indotta;
3- un'aumentata attività dell'enzima PAD4.

Per studiare meglio questo processo abbiamo messo a punto una tecnica di imaging intravitale nell'ulcera di modello murino, che parallelamente all'analisi citofluorimetrica

degli istoni citrullinati, ha messo in risalto il coinvolgimento della NETosi nel processo di guarigione delle ulcere diabetiche. Inoltre l'inibizione di PAD4 nel topo, ha dato evidenze sperimentali di un miglioramento nella guarigione delle ulcere.

In futuro questo protocollo sperimentale potrebbe essere utilizzato come strategia terapeutica di modulazione della NETosi per migliorare le DFU nei pazienti diabetici.

Introduction

Diabetes is one of the most common chronic diseases worldwide [1]. It is well known that diabetes mellitus (DM) affects blood cells. Altered susceptibility to infection of patients with diabetes has been ascribed to a depression in the function of polymorphonuclear (PMN) leukocytes. In diabetic patients with good glucose control, neutrophil function is slightly different than that of healthy ones. Diabetes causes significant changes in lymphocytes' metabolism and functions [2]. Increased risk of the occurrence of cardiovascular events is observed with the intensity of the inflammation which is reflected, among others, in elevated number of peripheral blood leukocytes. Attention is drawn to the higher rate of complications in patients with increased baseline leukocytosis. The correlation between the increase in leukocyte count and all-cause mortality is statistically significant. A higher risk of non-fatal myocardial infarction is also observed with the increase of leukocytosis. Neutrophils, which are the main pool of white blood cells, may play a role in these unfavorable phenomena [3].

Patients with diabetes, presenting with acute coronary syndrome, are at higher risk of cardiovascular complications and recurrent ischemic events in comparison to non-diabetic counterparts. Various mechanisms, including endothelial dysfunction, platelet hyperactivity, and abnormalities in coagulation and fibrinolysis have been implicated for this increased atherothrombotic risk [2].

Diabetes and DFU

415 million adults are estimated to currently have diabetes and there are 318 million adults with impaired glucose tolerance, which puts them at high risk of developing the disease in the future. By 2040 the number of people with diabetes is esteemed to rise to 642 million, of which 71 million only in Europe [4].

Diabetes is the most common cause of non-traumatic limb amputation in western countries [5]. Foot ulceration is a leading cause of hospital admissions for people with diabetes in the developed world and is a major cause of morbidity associated with diabetes, often leading to a poor quality of life for patients. Diabetic foot ulcers (DFUs) are estimated to occur in 15% of all patients with diabetes and precede 84% of all diabetes-related lower-leg amputations [6]. Most commonly, patients have neuropathy, which could be causative to DFUs. When coupled with an impaired ability to fight

infection, these patients become largely unable to mount the balanced inflammatory response that is required for wound healing. Thus, the DFUs could unleash an infection that can lead to sepsis and require limb amputation.

Several factors contribute to wound healing deficiencies in individuals with diabetes such as an impaired growth factor production and macrophage function, an altered collagen accumulation, a less vascularized granulation tissue, a dampened keratinocyte and fibroblast migration and proliferation, reduced number of epidermal nerves and a dysregulated balance between the accumulation of ECM components and their remodeling by MMPs [6] (see Figure 1).

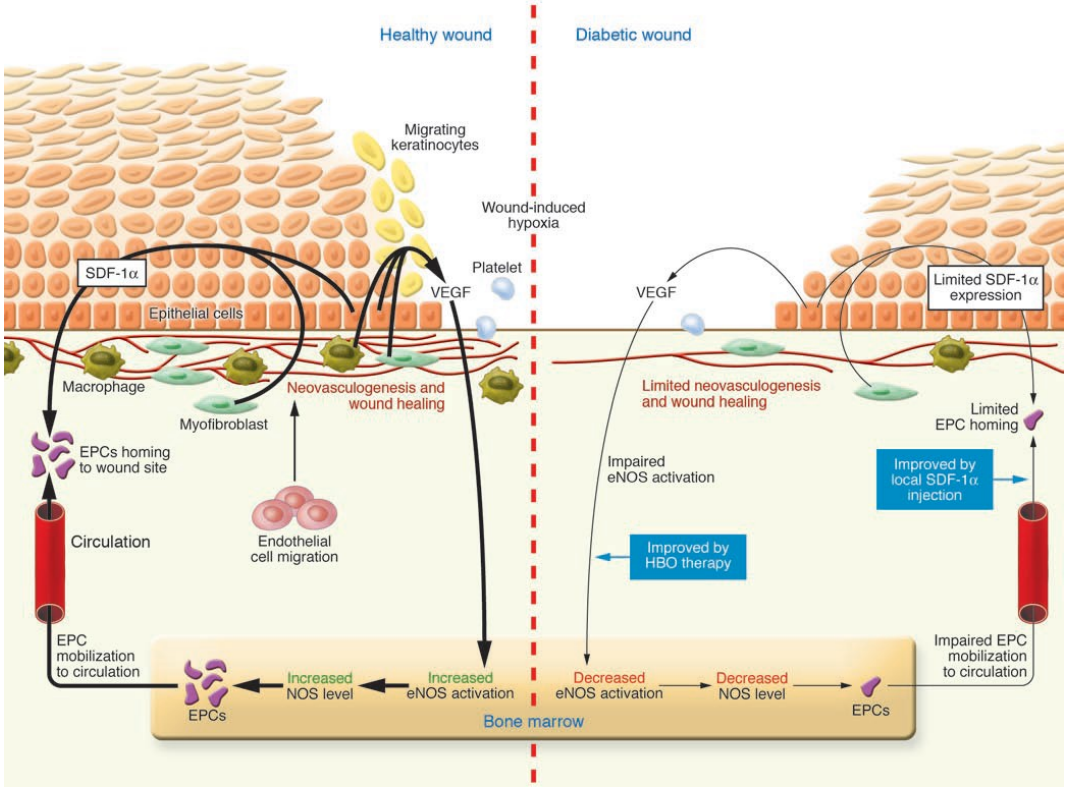

Figure 1 Mechanisms of wound healing in healthy people versus people with diabetes. In healthy individuals (left), the acute wound healing process is guided and maintained through integration of multiple signals (in the form of cytokines and chemokines) released by keratinocytes, fibroblasts, endothelial cells, macrophages, and platelets. During wound-induced hypoxia, VEGF released by macrophages, fibroblasts, and epithelial cells induces the phosphorylation and activation of eNOS in the bone marrow, resulting in an increase in NO levels, which triggers the mobilization of bone marrow EPCs to the circulation. The chemokine SDF-1a promotes the homing of these EPCs to the site of injury, where they participate in neovasculogenesis. In a murine model of diabetes (right), eNOS phosphorylation in the bone marrow is impaired, which directly limits EPC mobilization from the bone marrow into the circulation. SDF-1a expression is decreased in epithelial cells and myofibroblasts in the diabetic wound, which prevents EPC homing to wounds and therefore limits wound healing.

Wound repair

Regeneration and tissue repair processes consist of a sequence of molecular and cellular events which occur after the onset of a tissue lesion in order to restore the damaged tissue. All the events involved in wound repair can be divided into the following stages: inflammatory reaction, cell proliferation and synthesis of the elements which make up the extracellular matrix, and the posterior period, called remodeling. These stages are not mutually excluding, but rather overlap over time (Figure 2) [7].

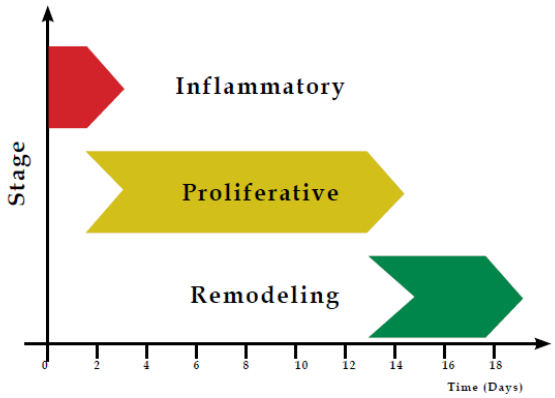

Figure 2 The 3 stages involved in tissue repaired. Image taken from [7].

The exudative, proliferative, and extracellular matrix remodeling phases are sequential events that occur through the integration of dynamic processes involving soluble mediators, blood cells, and parenchymal cells. Exudative phenomena that take place after injury contribute to the development of tissue edema. The proliferative stage seeks to reduce the area of tissue injury by contracting myofibroblasts and fibroplasia. At this stage, angiogenesis and re-epithelialization processes can still be observed. Endothelial cells are able to differentiate into mesenchymal components, and this difference appears to be finely orchestrated by a set of signaling proteins that have been studied in the literature. This pathway is known as Hedgehog [7].

In this thesis work, we focus the attention on the first phase in wound repairs, the inflammatory stage. In this phase, cell response is characterized by the influx of leukocytes in the wound area. Such a response is very quick and coincides with the key signs of inflammation, which are revealed by the edema and the erythema at the location of the lesion. Normally, cell response is established within the first 24 hours and can extend for up to two days. A quick activation of the immune cells in the tissue may also occur. Inflammation is a localized and protective tissue response that is unleashed by the lesion, causing tissue destruction [7]. Inflammatory cells play an important role in

wound healing and contribute to the release of lysosomal enzymes and reactive oxygen species, as well as facilitate the clean-up of various cell debris [8].

Neutrophils are among the first leukocytes to reach the wound after damage. Their canonical role is to eradicate bacteria and pathogens from the wound bed to be to kill microbes. This is usually achieved in phagolysosomes, but often results in neutrophils blitzing their environment with free radicals and other humoral factors that could kill host cells as well as the target infectious agents (this is particularly apparent in chronic wound situations) [9]. *Brinkmann et al [10]* have shown that another tactic for killing by neutrophils involves trapping microbes in *extruded NET*s of histones and DNA, process called *NETosis.*

Neutrophils and NETosis

Neutrophils, the most abundant leukocyte in the human body, have long been viewed as short-lived effector cells of the innate immune system, possessing limited capacity for biosynthetic activity and with a primary role in resistance against extracellular pathogens and in acute inflammation. These cells are characterized by their ability to act as phagocytic cells, to release lytic enzymes from their granules and to produce reactive oxygen intermediates (ROI) with antimicrobial potential. This view was challenged a few decades ago, by suggesting that neutrophils could survive much longer than first suggested [11]. Recently, it has been convincingly demonstrated that human neutrophils are short-lived, with a half-life of less than 1 day [12]. Latest evidence suggests that neutrophils can also produce anti-inflammatory molecules and factors that promote the resolution of inflammation [11]. The microbicide activity of neutrophils was known to be mediated by granule enzymes and oxidative burst, but it was recognized that activated neutrophils release granule proteins and chromatin that together form extracellular fibers that trap bacteria [10]. These so-called neutrophil extracellular traps (NETs) account for most of the ability of neutrophils to clear microorganisms. Release of nuclear material in NETs is followed by a type of cell death called NETosis.

It is still debated whether NETs release represents an active and specific physiological host defense mechanism or is simply a consequence of cellular rupture due to toxins or trauma. In 1996, neutrophil “suicide”, distinct from either necrosis or apoptosis, was described following chemical stimulation with phorbol myristate acetate (PMA). Fuchs

and colleagues [13] argued that PMA-induced DNA release could represent a novel host defense form of beneficial suicide, subsequently coined “NETosis.”

Neutrophils-generated NETs are structures composed of granule and nuclear constituents (proteolytic enzymes, antimicrobial proteins and ROS) that disarm and kill bacteria extracellularly. Notably, NETs are released only by activated neutrophils. Although naïve cells are round-shaped with some membrane folds (Figure 3 A and C), neutrophils stimulated with interleukin-8 (IL-8), PMA, or lipopolysaccharide (LPS) become flat and form membrane protrusions (Figure 3 B). Activated neutrophils but not naïve cells made prominent extracellular structures (arrows, Figure 3, B and D). These fibers, or NETs, are very fragile, and specimens need to be washed and fixed carefully to preserve them. High-resolution scanning electron microscopy (SEM) showed that the NETs contain smooth stretches with a diameter of 15 to 17 nm and globular domains of around 25 nm (Figure 3 E, arrowheads) that aggregate into larger threads with diameters of up to 50 nm. Analysis of cross sections of the NETs by transmission electron microscopy (TEM) revealed that they are not surrounded by membranes (Figure 3 F).

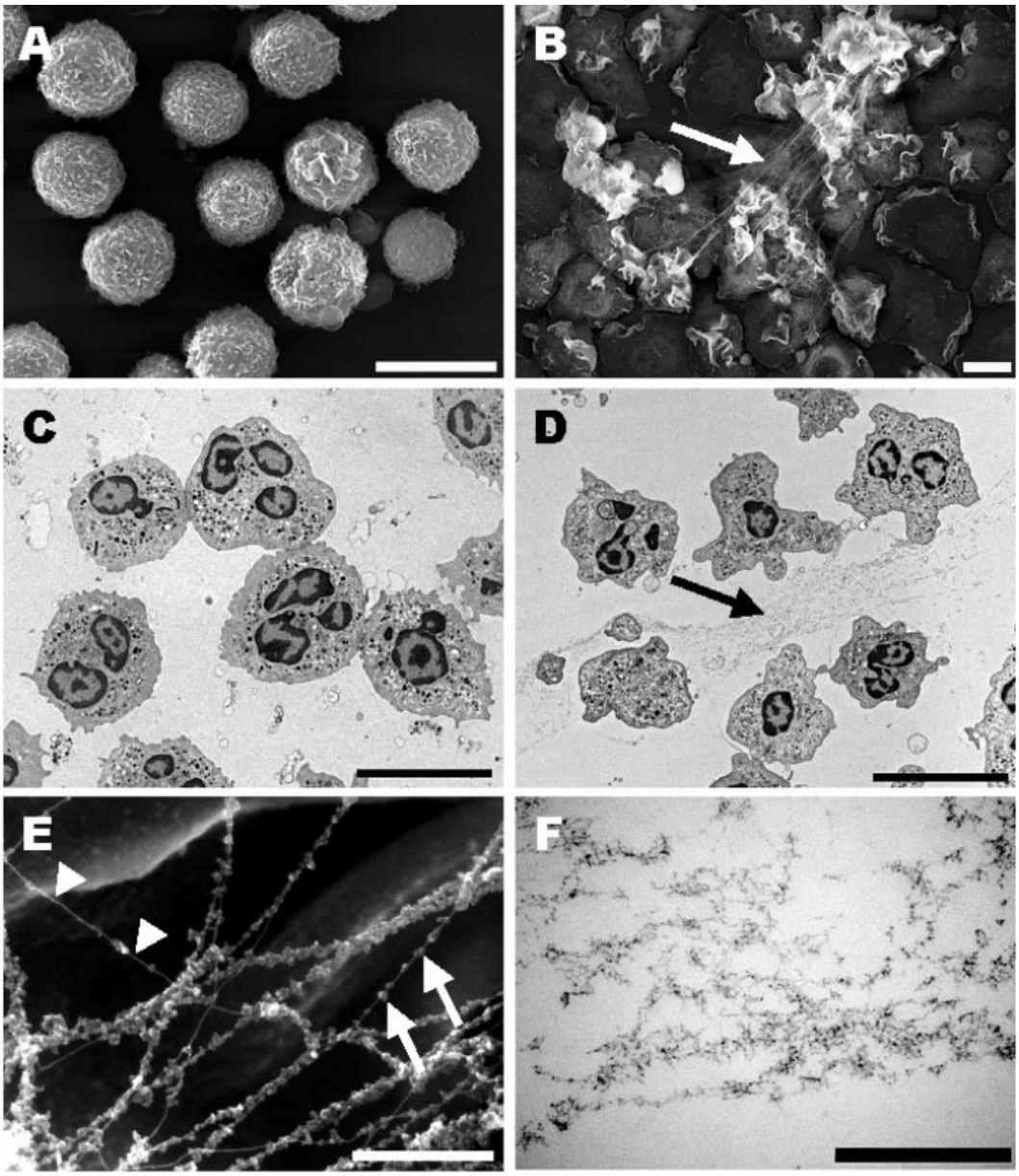

Figure 3 Electron microscopical analysis of resting and activated neutrophils. (A) Resting neutrophils are round and devoid of fibers. (B) Upon stimulation with PMA for 30 min, the cells flatten, make many membrane protrusions, and form fibers (NETs), arrows in (B) and (D). (C) TEM analysis of naïve neutrophils in suspension. (D) Ultrathin section of neutrophils stimulated in suspension with IL-8 for 45 min. Bars in (A) to (D) indicate 10 µm. The multilobular nuclei and different granules are clearly visible in both figures. The activated cells in (D) have many pseudopods and show NETs (arrow). (E) High-resolution SEM analysis of NETs that consist of smooth fibers (diameters of 15 to 17 nm, arrowheads) and globular domains (diameter around 25 nm, arrow). Globular complexes can be aggregated to thick bundles or fibers. (F) Ultrathin sections of NETs show that they are not membrane-bound. Neutrophils were stimulated as in (D). Bars in (E) and (F), 500 µm. Image taken from [10]

Molecular mechanism of NETosis

The events taking place during NETosis appear to follow a coordinated multi-step process that identifies a new type of programmed cell death: histone citrullination, chromatin decondensation, migration of elastase and other granule enzymes into the nucleus, disintegration of the nuclear membranes and release of DNA, histones and granule proteins into the extracellular space [14]. Owing to its negative charges, DNA forms the sticky backbone of NETs, onto which histones and enzymes attach (Figure 4). These filaments organize in networks that physically entrap bacteria, but also allow the local concentration of bactericidal components, that could not be possible if they were freely released in the extracellular fluid, whence they would be rapidly cleared [14]. DNA fibers are decorated with several proteins like neutrophil elastase (NE), myeloperoxidase (MPO), cathepsin G, proteinase 3 (PR3), high mobility group protein B1 (HMGB1), and LL37, thus displaying proinflammatory characteristics [15].

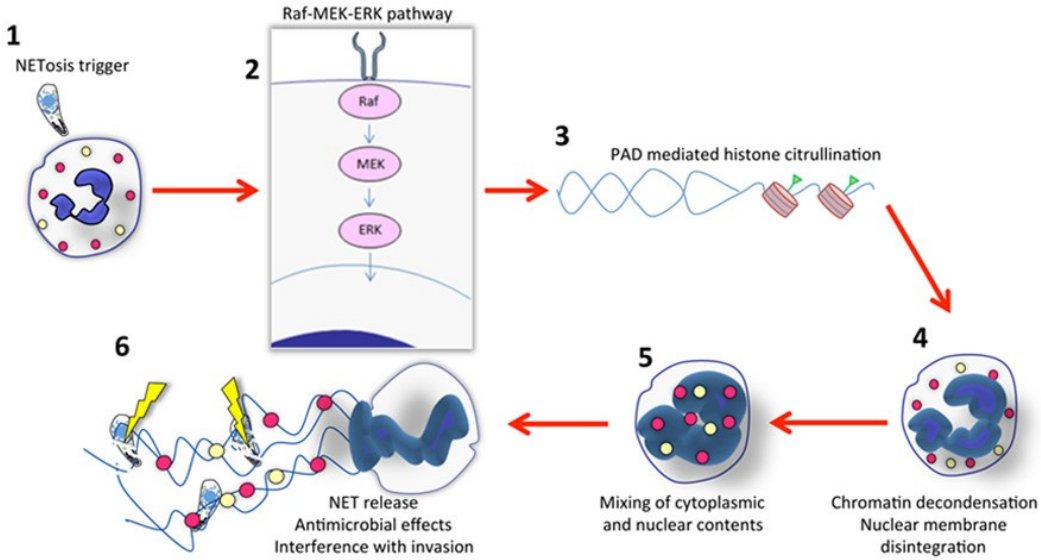

Figure 4 Outline of NET formation. (1) Initiation of NETosis generally occurs through engagement of cell surface receptors. While invasion itself is not required, it is possible that adhesion enables high local concentrations of parasite ligands that trigger the NET cascade. (2) Evidence indicates involvement of the Raf–MEK–ERK pathway during NET formation elicited by several stimuli. In most cases, NADPH oxidase is also involved. (3) Signaling to the nucleus results in chromatin modification. Histone citrullination mediated by peptidyl arginine deiminase (PAD)appears to be a prerequisite for NET release. (4) Concurrent with chromatin decondensation, the nuclear membrane disintegrates. (5) This results in mixing of cytoplasmic, granule (yellow and red circles) and nuclear contents. (6) Finally, DNA with associated histones and granule molecules are released into the extracellular environment entrapping microbes in the vicinity. Image taken from [16]

Citrullination is the conversion of positively charged arginine side chains into polar but uncharged citrulline side chains, by deimination. Of the five-known human peptidylarginine deiminases (PADs) known to catalyze such conversions, PAD4 is the most extensively studied isoform. It is expressed by various leukocytes, including

neutrophils and immuno-modulatory functions have been ascribed to PAD4 activity. Like other PAD isotypes, PAD4 is a Ca^{2+} dependent enzyme, but only PAD4 possesses a classical nuclear localization signal (NLS). Importantly, the citrullination of nuclear histone H3 has been reported to counteract transcription by preventing the methylation of arginine. In neutrophils, inhibition of PAD4 prevents citrullination of histone H3 and significantly reduces NETs release induced by a Ca^{2+}-ionophore or *Shigella flexneri* bacteria in differentiated HL60 cells. These data suggest that nuclear histones have a regulatory role during NETosis in addition to their direct antimicrobial role [17].

In 2007, it was reported that, going along with chromatin decondensation, neutrophils undergo an NADPH oxidase-dependent death process that includes nuclear envelope disintegration and the mixing of nucleic acids and granule proteins within a large intracellular vacuole [13]. This is followed by plasma membrane rupture and the release of chromatin, decorated with granular proteins, into the extracellular space. In vitro NETosis is completed in 1 to 4 h after the triggers were added to neutrophils [15].

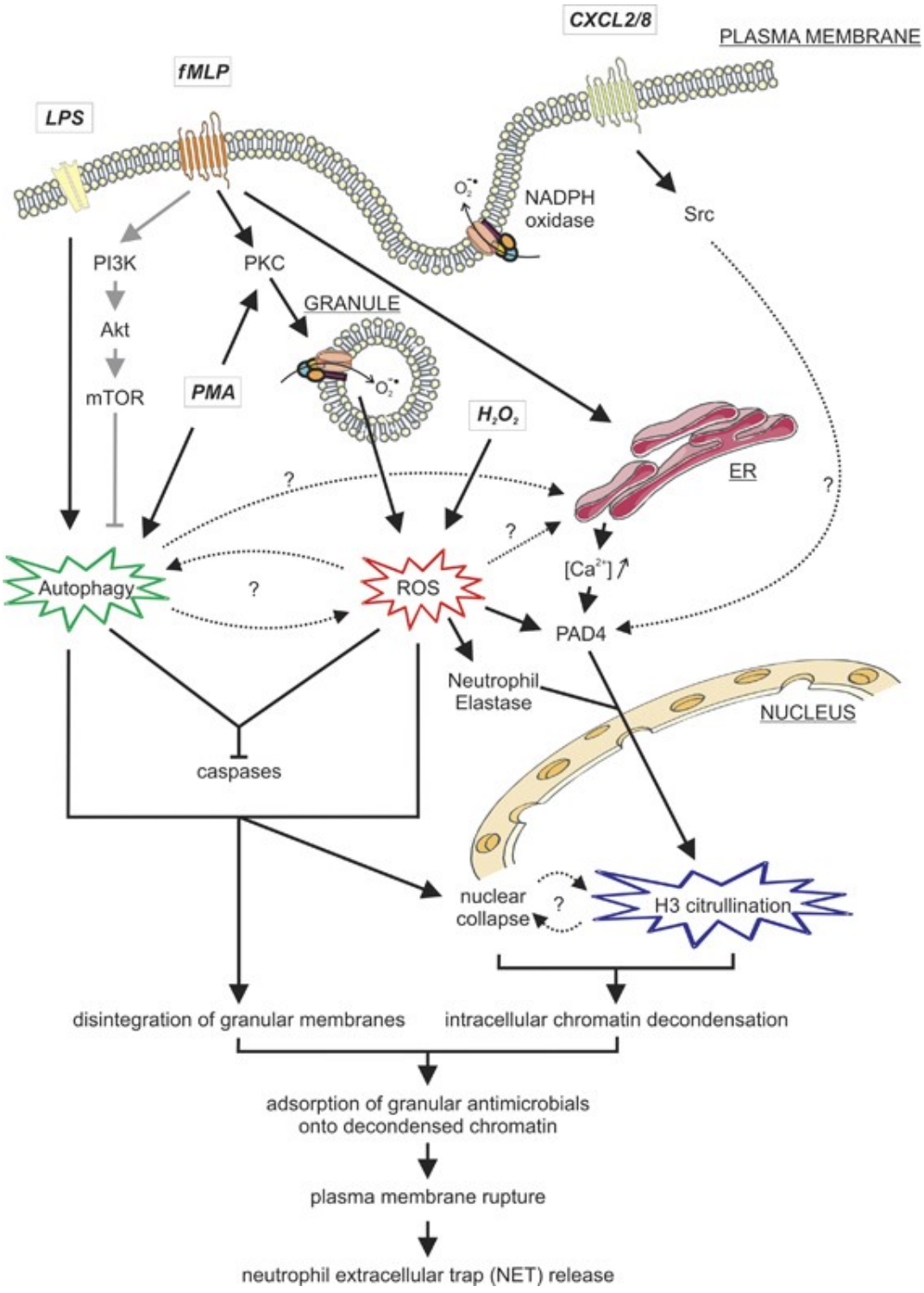

Figure 5 Triggers and steps of NETosis. This Figure was produced using Servier Medical Art: www.servier.com

It is reported that treatment with pro-inflammatory stimuli, such as LPS, IL-8, fMLP (N-Formylmethionyl-leucyl-phenylalanine) or *Shigella flexneri* induces a marked increase in the citrullination of histone H3.

The cascade of events in the intracellular signaling pathway that follows is poorly known, but it culminates in the activation of NADPH oxidase (NOX), as the

compartmentalized NOX-dependent oxidative burst is one main feature of NETosis [17]. *In vitro*, NETosis is typically stimulated by the protein kinase C (PKC) PMA. In turn, PKC is responsible for membrane translocation and assembly of the NOX complex to allow neutrophil respiratory burst [18]. The importance of NOX in NETosis is highlighted by the finding that patients with chronic granulomatous disease, who carry mutations in NOX components, show a severe deficiency in NETs release, which can contribute to their susceptibility to infections. Other features of this PMA-inducible NOX-dependent NETosis are activation of ERK1/2, p38 MAP kinase, Akt, and the autophagic machinery. Activation of Akt, in particular, is believed to shift balance between apoptosis and NETosis toward the latter in neutrophils. In addition, a NOX-independent NETosis pathway has been recently described, which can be induced by calcium ionophores (e.g. ionomycin and a23187) and is mediated by small conductance potassium (SK3) channels and mitochondrial ROS [19].

Bacterial damage-associated molecular pattern (DAMPs), such as LPS, are known triggers of autophagy in many cell lines, including neutrophils. However, purified LPS does not activate NADPH oxidase directly, but only sensitizes for a more powerful NADPH oxidase-derived oxidative burst induced by a subsequent trigger of NADPH oxidase. Formylated oligo peptides, like fMLP, are potent triggers of NADPH oxidase. Consequently, fMLP activates NADPH oxidase as well as Histone H3 citrullination. However, fMLP does not induce NETosis. The fMLP induces signaling through Akt/PI3K as well. This cascade PI3K/Akt/mTOR may inhibit autophagy and thereby prevent NETosis. Both reactive oxygen species (ROS) production and H3 citrullination are insufficient to mediate the collapse of the nuclear membrane. Accordingly, hydrogen-peroxide (H_2O_2) only accelerates neutrophil apoptosis. Induction of autophagy without NADPH oxidase activity also results in enhanced apoptosis, with no signs of NETosis. However, ROS, which are sufficient to induce consequent H3 citrullination, in combination with induced autophagy leads to chromatin decondensation and collapse of the nuclear membrane and prevents the activity of executioner caspases (Figure 5).

Ca^{2+} flux is necessary for efficient NET formation, and its role does not seem to be restricted to the generation of ROS, but also promotes histone citrullination by PAD4; PAD4 is a Ca^{2+}-dependent enzyme, that is key in mediating NETosis [20]. The activation of protein kinase C (PKC) by PMA has also been shown to be important, and appears to

depend on phosphorylation of p38 MAPK and ERK, by a pathway that may suppress apoptosis to permit NETosis [21].

Downstream Ca^{2+} signaling induced by IL-8 in neutrophils occurs in two phases: a rapid initial release from intracellular stores, mainly from the endoplasmic reticulum via the activation of phospholipase Cβ (PLC) and the subsequent action of IP3, followed by a prolonged influx mediated by the activation of Ca^{2+} release activated Ca^{2+} (CRAC) channels. A graphical summary of the potential signal-transducing cascade is provided in Figure 6.

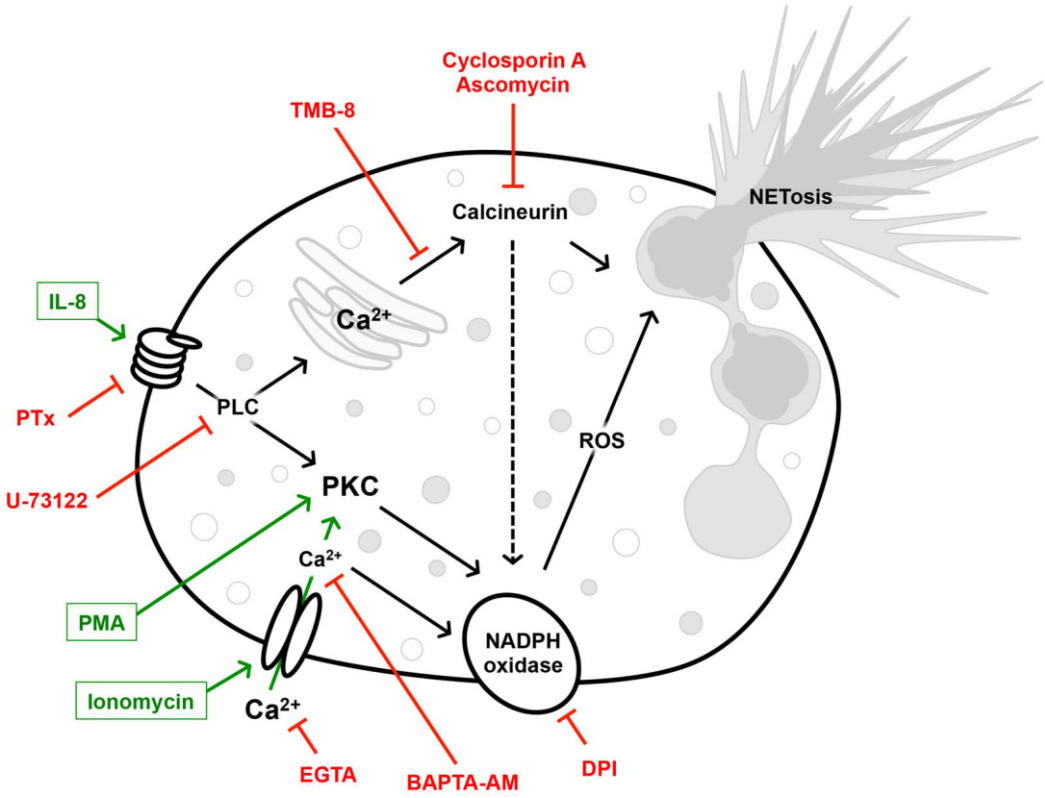

Figure 6 Schematic representation of the Ca^{2+}-dependent signal transduction pathway of NETosis. Image taken from [21].

NETosis: a distinct cell death program

NETosis is distinct from necrosis, apoptosis, necroptosis and autophagy: though some characteristics of NETosis can be found in other types of cell death, such as membrane degradation and Ca^{2+} overload, other features are quite specific.

In contrast to apoptotic cells, NETotic cells do not display eat-me signals such as phosphatidyl serine (PS) before plasma membrane disruption, preventing their clearance by phagocytes (Figure 7). Live cell imaging of healthy neutrophils stimulated

with 100 nM PMA reveals a cell death program characterized by immediate cell flattening and increased adherence, followed by loss of mitochondrial membrane potential and induction of vacuolization [22]. Differently to apoptosis or programmed necrosis (necroptosis), both the nuclear and granular membranes disintegrate during NETosis, but plasma integrity is maintained. This allows the antimicrobial granular cargo to mix with nuclear chromatin. No morphologic signs of apoptosis are observed, such as membrane blebbing, nuclear chromatin condensation, PS exposure before plasma membrane rupture and internucleosomal DNA cleavage [17].

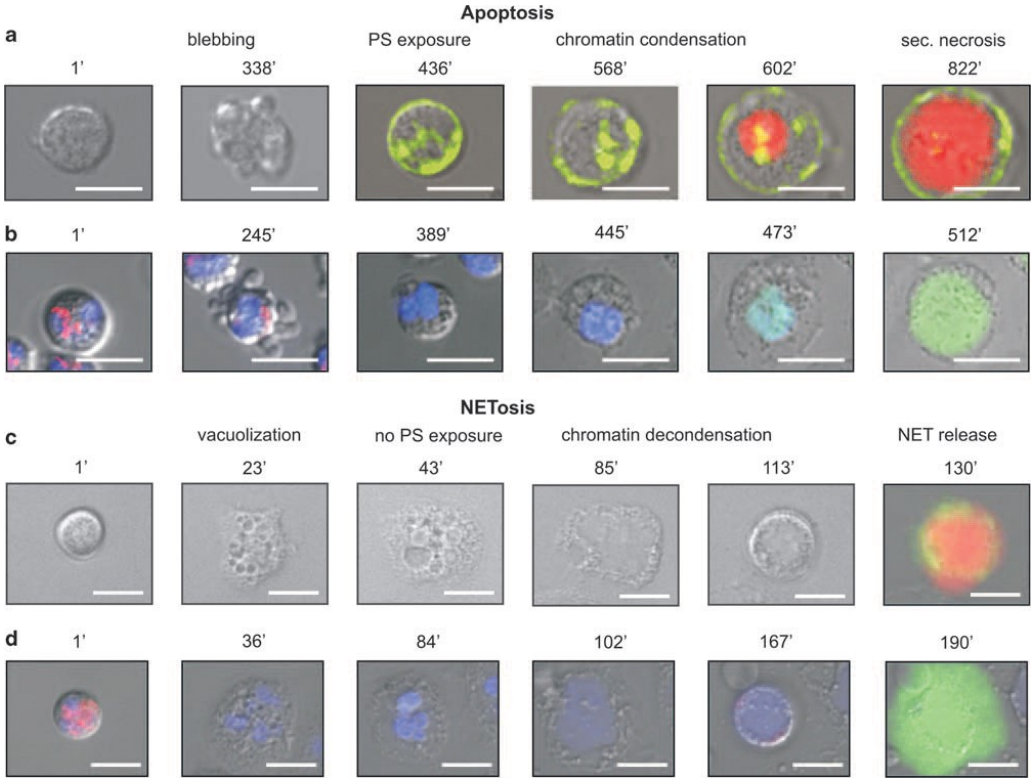

Figure 7 Live cell imaging of subcellular events during ex vivo neutrophil apoptosis and NETosis. (a and c) Cells were incubated with Alexa488-AnnexinV (green) and the cell-impermeable DNA dye propidium iodide (red), (b and d) or with the cell impermeable DNA dye Hoechst (blue), the mitochondrial membrane potential marker TMRM (red) and the cell impermeable DNA dye, propidium iodide (green). Constitutive neutrophil apoptosis is characterized by membrane blebbing, PS exposure (green) and condensation of nuclear chromatin (blue); cells finally undergo secondary necrosis. During induced NETosis, cells display massive vacuolization and decondensation of nuclear chromatin (blue), and PS is not exposed (green) before NET formation (green). Scale bars indicate 10 mm. Image taken from [17]

PMA induces typical features of NETosis, which differs both biochemically and morphologically from apoptosis and necrosis. Remijsen and colleagues [22] confirmed by live cell imaging of PMA-stimulated healthy neutrophils, that NETosis is characterized by: immediate cell flattening and increased adherence, loss of mitochondrial membrane potential and induction of massive vacuolization (Figure 8 A). Vacuolization is observed for up to 90-130 min after PMA stimulation, until the nuclear envelope disintegrates and nuclear chromatin decondenses, which allows it to mix with the cytoplasmic content.

During all that time, plasma membrane integrity is preserved. After 140 min, the plasma membrane permeabilizes and decondensed chromatin is released. Figure 8 B shows the mean percentage of cells undergoing to these different subcellular events from a kinetic analysis of 150 cells from four independent experiments. Mitochondrial depolarization is not a crucial mediator of DNA decondensation. In this regard, it is noteworthy that neutrophils depend on glycolysis instead of oxidative phosphorylation to meet their energy demands.

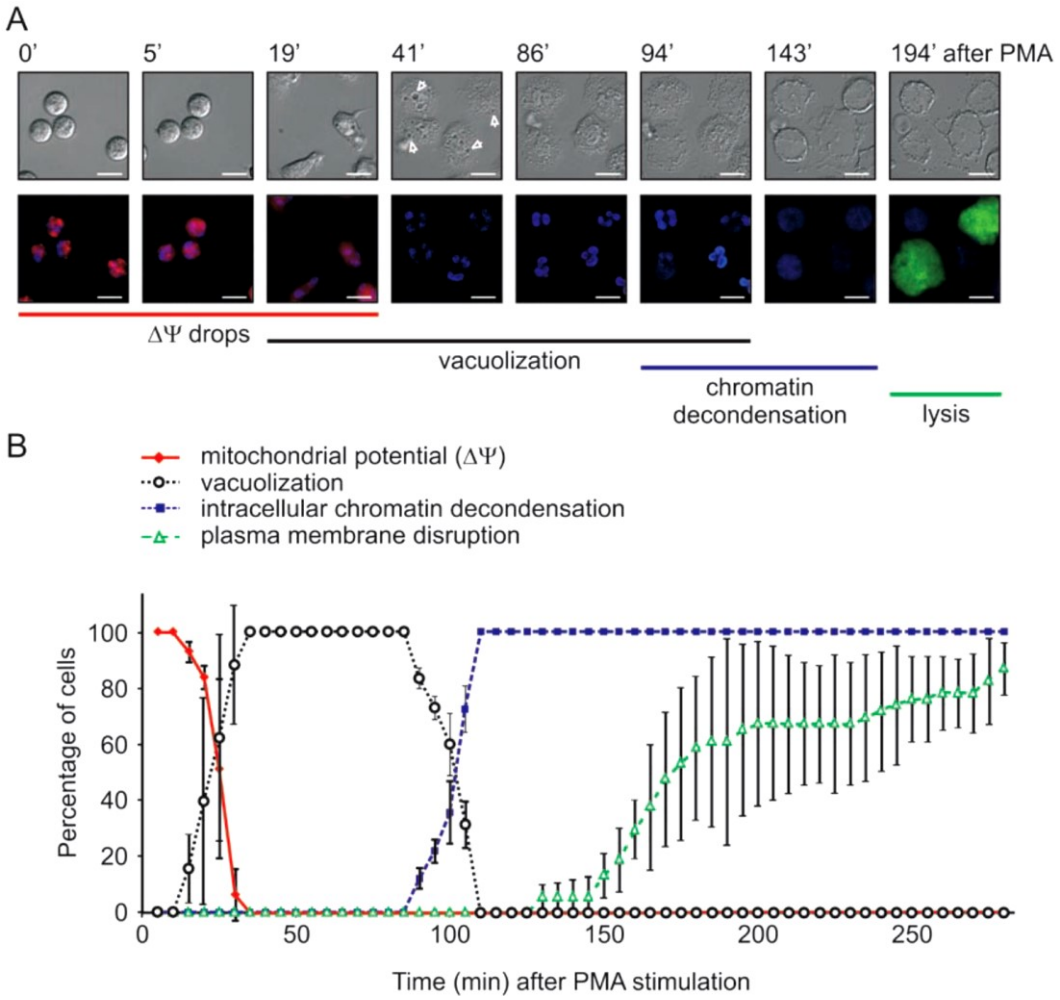

Figure 8 PMA-induced NETosis is characterized, chronologically, by cell flattening and adherence, a drop in mitochondrial membrane potential, vacuolization and intracellular chromatin decondensation. (A) Isolated neutrophils were monitored by live cell imaging. (B) Kinetic analysis of 150 neutrophils.

NETosis differs also from another regulated cell death mechanism, which will be described followed and is called necroptosis. This process is well defined as a viral defense mechanism, allowing the cell to undergo "cellular suicide" in a caspase-independent fashion in the presence of viral caspase inhibitors [23]. Necroptosis is similar to apoptosis, however there are some differences, which are schematically represented in Figure 9.

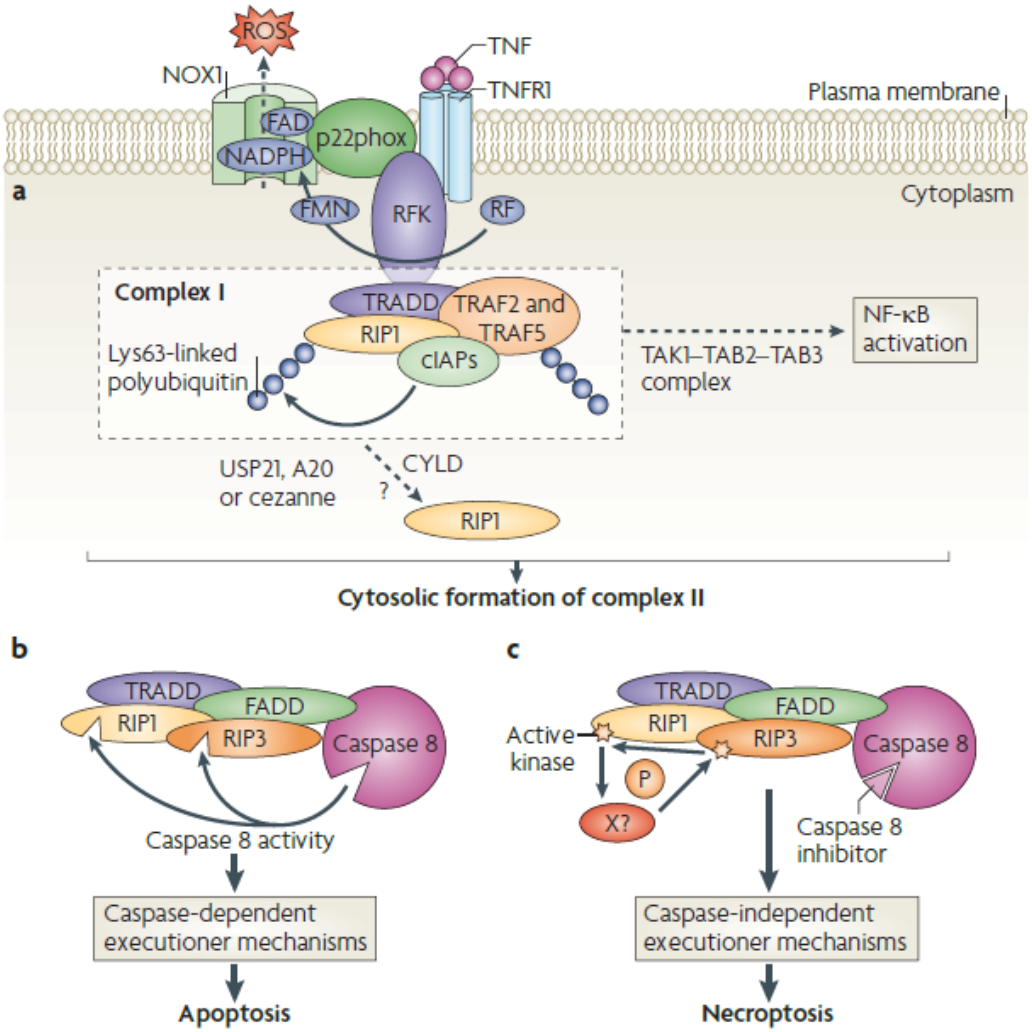

Figure 9 TNFR1-elicited signaling pathways. (A) On TNF binding, TNFR1 undergoes a conformational change, allowing for the intracellular assembly of the so-called TNFR complex I, which includes TNF receptor-associated death domain (TRADD), receptor-interacting protein 1 (RIP1; also known as RIPK1), cellular inhibitor of apoptosis proteins (cIAPs), TNF receptor-associated factor 2 (TRAF2) and TRAF5. On cIAP-mediated Lys63-ubiquitylation, RIP1 can serve as a scaffold for the recruitment of transforming growth factor-β activated kinase 1 (TAK1), TAK1-binding protein 2 (TAB2) and TAB3, which initiate the canonical nuclear factor-κB (NF-κB) activation pathway (BOX 2). Riboflavin kinase (RFK) physically bridges the TNFR1 death domain to p22phox (also known as CYBA), the common subunit of multiple NADPH oxidases, including NADPH oxidase 1 (NOX1), which also contributes to TNFα-induced necroptosis by generating reactive oxygen species (ROS). Conversely, on deubiquitylation by cylindromatosis (CYLD; and perhaps also by A20 (also known as TNFAIP3), cezanne (also known as OTUD7B) or ubiquitin-specific peptidase 21 (USP21)), RIP1 exerts lethal functions, which can be executed by two distinct types of cell death. (B) The internalization of TNFR1 is accompanied by a change in its binding partners that leads to the cytosolic assembly of TNFR complex II, which often (but not invariably) contains TRADD, FAS-associated protein with a death domain (FADD), caspase 8, RIP1 and RIP3 (also known as RIPK3). Normally, caspase 8 triggers apoptosis by activating the classical caspase cascade. It also cleaves, and hence inactivates, RIP1 and RIP3. (C) If caspase 8 is blocked by pharmacological or genetic interventions, RIP1 and RIP3 become phosphorylated and engage the effector mechanisms of necroptosis. FAD, flavin adenine nucleotide; FMN; flavin mononucleotide. Image taken from [24].

In contrast to constitutive or anti-Fas-induced neutrophil apoptosis, PMA-induced NETosis was insensitive to the pan-caspase inhibitor benzyloxycarbonyl-Val-Ala-Asp(Ome)-fluoromethylketone (zVAD-fmk). Caspase activity is only detected during spontaneous neutrophil apoptosis, but not during PMA induced NETosis. Moreover, the

kinetics of PMA-induced NETosis are not affected by treatment with zVAD-fmk (Figure 10 A). These findings could exclude the involvement of caspases in NETosis.

NETosis process is different also to necrosis. Several necrostatins have been identified by virtue of their ability to suppress necrosis induced by TNF. The inhibition of programmed necrosis by pretreatment with necrostatin-1 (Nec-1), an inhibitor of RIP1 kinase activity, also does not affect the kinetics of PMA-induced NETosis [22] (see Figure 10 C).

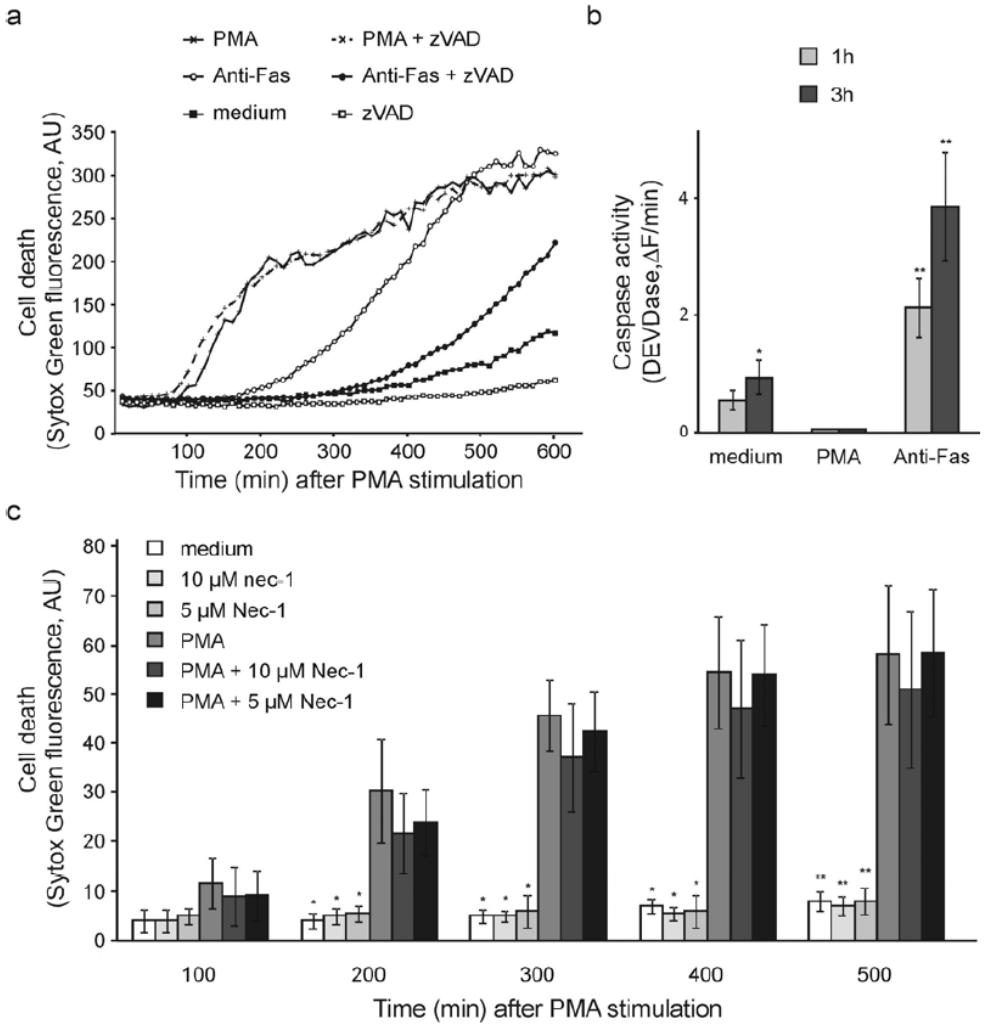

*Figure 10 PMA-induced NETosis differs from neutrophil apoptosis and necroptosis. (A) In the presence of 50 nM Sytox Green, 2 x105 neutrophils were incubated with or without 10 µM zVAD-fmk for 30 min. They were left unstimulated or were stimulated with 100 nM PMA or 250 ng/ml anti-Fas antibody for the indicated times. Cell death was detected by measuring the fluorescence of the cell impermeable DNA dye Sytox Green. Data are expressed as mean Sytox Green fluorescence ± SD (n= 3), as percentage of maximal Sytox Green fluorescence. zVAD-fmk significantly inhibited anti-Fas stimulated DNA release, whereas zVAD-fmk did not significantly inhibit PMA-induced DNA release. (B) Protease activity against the caspase substrate DEVD-amc was determined. Data are expressed as the mean ΔF/min ± SD (n=3). *, p< 0.05 and **, p< 0.001, as compared to PMA-stimulated neutrophils. (C) Neutrophils (2 x105) were incubated with or without 5 or 10 µM Nec-1 for 30 min, and either left unstimulated or were stimulated with 100 nM PMA for the indicated durations, in the presence of the cell impermeable DNA dye Sytox Green (50 nM). Data are expressed as percentage of maximal Sytox Green fluorescence ± SD (n=4) as a function of time. *, p< 0.01, as compared to PMA stimulated normal neutrophils. Image taken from Supplementary [22].*

Suicidal NETosis vs vital NETosis

In 1996, neutrophil suicide, distinct from either necrosis or apoptosis, was described following chemical stimulation with PMA [25]. The potential importance of this observation went unrecognized until the Zychlinsky laboratory reported that PMA-induced suicide resulted in the release of a novel host defense structure, named NETs [10].

This classical "suicidal" NETosis occurs *in vitro* following stimulation by PMA through activation of protein kinase C and the RAF–mitogen-activated protein kinase (MEK)–extracellular signal-regulated kinase (ERK) pathway. NADPH assists in the translocation of neutrophil elastase from cytosolic granules into the nucleus where it aids in chromatin breakdown via histone cleavage. MPO is required for chromatin and nuclear envelope breakdown and granular mixing within the NET vacuole. Following 120 min of intracellular NET formation, the neutrophil outer membrane ruptures, and the mature NET is extruded (Figure 11 A-C). On the other hand, Yipp et al [26] have provided evidence of a "vital" NETosis pathway distinct from suicidal NETosis, where neutrophils after the release of NET are alive.

Vital NETosis has been reported following both direct microbial exposure and LPS. Live S aureus induce rapid NET release (<30 minutes) in human and mouse neutrophils *in vitro* and *in vivo*. For gram-negative bacteria, NETs are induced via Toll-like receptor (TLR) 4 activation of platelets followed by direct neutrophil-platelet interaction via CD11a, whereas both complement receptor 3 and TLR2 are required for vital NETosis following gram-positive infection (Figure 11 D-F) [26].

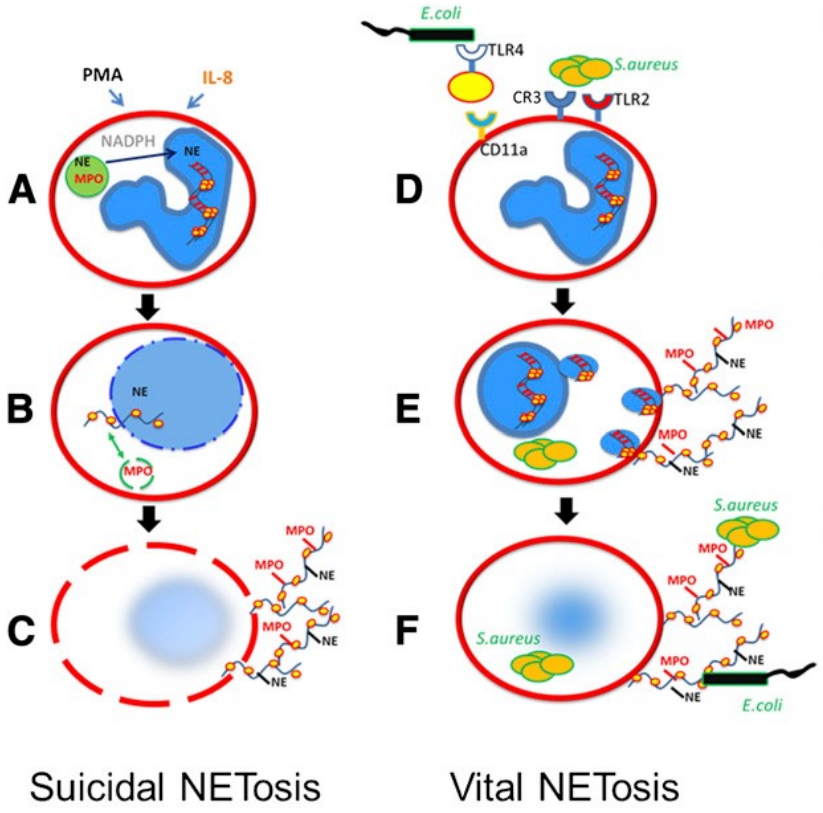

Figure 11 The comparison of two different mechanisms of conventional suicidal NETosis vs vital NETosis. Image taken from [26]

NETosis in diabetes

Constitutively active innate immune responses are associated with pathophysiological conditions of several diseases such as diabetes and obesity, autoimmune, neurodegenerative disorders and thrombosis related diseases. As an essential component of innate immune system, neutrophils play an important role by inducing hyper-responsive pro-inflammatory milieu during the pathogenesis of such diseases [27].

Whereas type 1 diabetes is characterized by autoimmune destruction of pancreatic islets, type 2 diabetes (T2D) has been described as an autoinflammatory disorder, characterized first by insulin resistance in peripheral tissues followed by beta cell failure, including decreased islet size and insulin production.

Chronic low grade tissue inflammation is an important cause of systemic insulin resistance, and is a key component of the decreased insulin sensitivity which exists in obesity and T2D. Immune cells such as macrophages, T–cells, B–cells, mast cells and

eosinophils have all been implicated as playing a role in this process. Neutrophils are the first immune cells to respond to inflammation, and can promote a more chronic inflammatory state by helping to recruit macrophages and interacting with antigen presenting cells [11].

A dysregulation in NETosis can represent a hitherto neglected link among hyperglycemia, oxidative stress, inflammation and diabetic complications, for 3 reasons: (1) diabetes affects neutrophil count and activity, (2) hyperglycemia-driven oxidative stress paves the way to diabetic complications and (3) neutrophils generate oxidative stress in diabetes. Under diabetic conditions, neutrophils produce more superoxide and cytokines than in normoglycemic conditions. Tumor necrosis factor-α (TNF-α), which primes neutrophils for NETs release, is increased in diabetic individuals [28]. The diabetic microenvironment may thus facilitate NETosis [20]. Indeed, our laboratory [29] has recently reported that high glucose in vitro and hyperglycemia in patients with diabetes increased NETosis and its surrogate markers, respectively.

Increased NETosis in diabetes suggests that NETs may play a role in diabetic complications, and that inhibiting NETosis or cleavage of NETs may lessen them [20]. Local infection, which is common in DFU, triggers neutrophil activation and the release of NETs composed of granular proteins/enzymes and nuclear material, such as DNA and histones complexed in chromatin [17]; however, excess or deregulated NETosis can cause tissue damage. Wong et al. [20] found that PAD4, the key enzyme triggering NETs release, is overexpressed in diabetes, and NETosis induction can be demonstrated in murine models of DFU. Remarkably, the inhibition of NETosis by PAD4 knock-out or disruption of NETs with DNase-1 accelerated wound healing.

Aim

The aim of this work is to study the role of NETosis in delayed diabetic wound healing in humans. To accomplish that we coupled data generated from proteomic analysis of DFU with in vivo model of diabetic ulcers analyzed with intravital microscopy. Furthermore, we deployed a custom-build two-photon microscopy to study and dissect the single step of NETosis *in vitro*. A better comprehension of cellular and molecular mechanisms that delay tissue healing in diabetes could help for new therapeutic strategies beyond glucose control, revascularization, and traditional wound care.

Material and methods

Multiphoton microscopy

The development of multi-photon intravital microscopy has been a breakthrough technique for deep-tissue imaging of dynamic cell behavior inside live organisms [30].

The Multi-Photon Microscopy (MPM) is a form of laser-scanning microscopy, which represents the best non-invasive imaging technique. MPM shows several advantages compare to convention confocal imaging: high resolution, reduced signal-loss due to light scattering from the regions above the focal plane, and the possibility to reach 1 μm depth [31].

The acquisitions of all the experimental data were performed with a costume-made two-photon microscope (Bergamo II, Thorlabs), which was designed in collaboration with Prof. Fabio Mammano (CNR, Rome) e Prof. Filippo Romanato (University of Padua). It is equipped with 8 kHz resonant scanner, extended-field-of-view collection optics, 4 independent detection channels in the backward direction and laser-scanned Dodt contrast in the forward direction. The microscope was coupled to two synchronized pulsed laser beams generated by a Ti:Sapphire pump laser (Chameleon Ultra 2, Coherent) and an optical parametric oscillator (Camelion Compact OPO).

Two-photon microscopy at 800 nm excitation was used to visualize simultaneously 4 channels: green channel, blue channel, red channel and gray channel (transmitted light, for *in vitro* cell structure, or SHIM *in vivo*). SHIM or Second-Harmonic Imaging Microscopy is an imaging technique, which is based on nonlinear optical effect known as second-harmonic generation (SHG) and it allows us to visualize cell and tissue structure and function, like collagen or microtubule. Experiments were performed with a 60x objective (Olympus LUMFLN60XW, N.A. 1.1, 1.5 WD) or a 25x objective optimized for multiphoton imaging (Olympus XLPLN25XWMP2, N.A. 1.05, W.D. 2 mm).

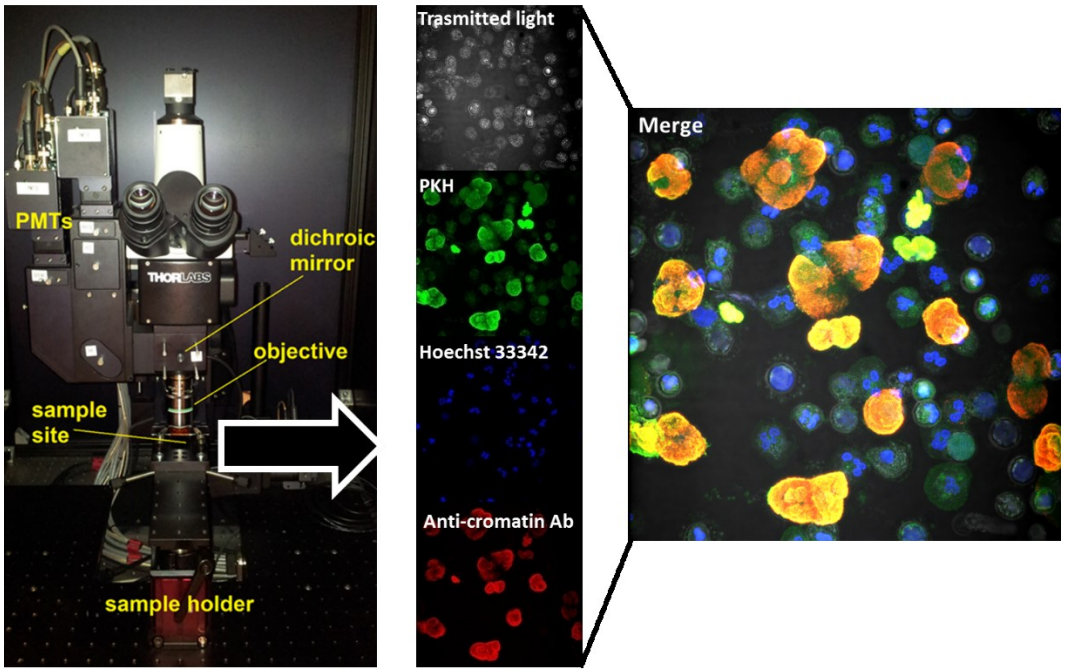

Figure 12 On the left, our two-photon microscope; in the center, an example of NETosis imaging represents in all channels, taken simultaneously; on the right, a merge of all channels.

Isolation of human neutrophils, stimulation of NETosis and in vitro *imaging*

Neutrophils were isolated from EDTA-treated peripheral blood of healthy subjects using an immune-magnetic isolation kit, which yielded a highly pure neutrophil population (MACSxpress Human Neutrophil Isolation Kit, Miltenyi Biotec).

We stained neutrophils using different dyes, the characteristics of which are summarized in Table1.

Table 1

Channel	Dye	Concentration	Incubation timing at 37°C	Target
Blue channel (460/50nm)	Hoechst 33342 (cell-permeable)	1 µg/mL	5 min	Nuclear dsDNA
Green channel (525/40nm)	Sytox green (cell-impermeable)	100 nmol/L	Immediately in the medium	Extracellular dsDNA in NETs
	Fluo-4	10 µM	20 min + 20 min washing	Intracellular calcium
	ROS dye	50 µM	30 min	Intracellular ROS
	PKH green	4 µM	5 min	Cellular membrane
	Alexa488-polyclona-rabbit anti-human elastase	1:200 Stock	1h	Elastase
Red channel (625/90)	Tetramethylrhodamine (TMRM)	50 nmol/L	5 min	Energized mitochondria
	AnnexinV	1:1000 Stock	1 h	Phosphatidyl serine
	Cy3-coniugated Antihuman PL2-3 monoclonal antibody	1:200 Stock	Immediately in the medium	Subnucleosomal complex of Histone 2A, 2B and chromatin

To stimulate NOX-dependent NETosis, neutrophils were incubated with phorbol 12-myristate-13-acetate (PMA) [100 nmol/L] at 37°C and 5% CO2 for 2 h. For stimulation of NOX-independent NETosis, neutrophils were incubated with calcium ionophores (a23187 at 25 µM concentration, and ionomycin at 5 µM concentration).

The experiments were performed with an Olympus 60x objective.

Animals

All procedures were approved by the local ethics committee and from the Italian Ministry of Health. Experiments were conducted according to the National Institutes of Health Principles of Laboratory Animal Care. We used 30 wild-type C57Bl/6J mice (Jackson Laboratory), fed a standard diet containing 10% of energy from fat.

Diabetes was induced with a single i.p. injection of streptozotocin (150 mg/kg, Sigma Aldrich) in citrate buffer pH 4.5. Glycaemia was measured with a commercially available glucometer (Abbott) and animals with blood glucose ≥300 mg/dl were housed for 4 weeks before performing the experiments.

To induce hind limb wounding, 10 animals were sedated with inhaled isoflurane (Abbott) and the lateral portion of the tight was shaved with Veet® cream. After skin disinfection, a 4 mm-round excisional full-thickness wound was performed with a skin biopsy punch (Kai Medical, Japan). Digital photographs of the wounds were taken at pre-specified time points with a reference ruler to estimate wound area, that was calculated with ImageJ software (NIH). To ensure PAD4 inhibition, Cl-amidine (Merck Millipore) was injected daily subcutaneously at 10 mg/kg (in DMSO) for 1 week before performing excisional wounds and continued throughout healing. Control group received daily injection of the vehicle (DMSO).

Intravital imaging

10 mice were sedated with zolazepam/thylamine and xylazine, placed on a custom-made holder, and positioned under an Olympus 25x objective. Wounds were evaluated at day 3. Thirty minutes before imaging, mice were intravenous (i.v.) injected with 5 µL Sytox green, 3 µL phycoerythrin-conjugated anti-mouse Gr-1, and 50 µL Hoechst 33342. In separate experiments, the vasculature of mice was stained by injecting i.v. 50 µL of a 10 mg/dL solution of high–molecular weight (150 kDa) fluorescein isothiocyanate (FITC)–conjugated Dextran.

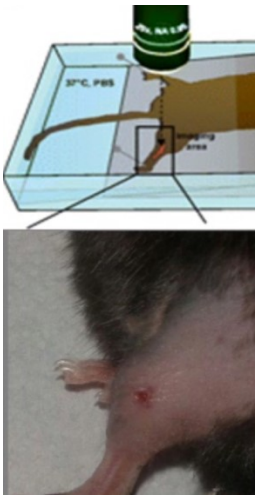

Figure 13 Setting to allows us the visualization of ulcer in mice.

Wound healing in mice

To ensure PAD4 inhibition, Cl-amidine (Merck Millipore) was injected daily subcutaneously at 10 mg/kg (in DMSO) for 1 week before performing excisional wounds and continued throughout healing. Control group received daily injection of the vehicle (DMSO).

Animals were sedated with inhaled isoflurane (Abbott) and the lateral portion of the tight was shaved with Veet® cream. After skin disinfection, a 4 mm-round excisional full-thickness wound was performed with a skin biopsy punch (Kai Medical, Japan). Digital photographs of the wounds were taken at pre-specified time points with a reference ruler to estimate wound area, that was calculated with ImageJ software (NIH).

Data and Statistical Analysis

We used ImageJ/Fiji software (1.48r, NIH, USA) to process raw data files. We registered in different two ways: 1) z-stack recording (or focal plane merging and z-stacking or focus blending), which is a digital image processing technique which combines multiple images taken at different focus distances to give a resulting image with a greater depth of field than any of the individual source images; 2) streaming recording, which simultaneously take 4 channels during pre-fixed period.

Proteomic Analysis

Our laboratory has previously developed and validated a proteomic platform for identification of biomarkers and new molecular mechanisms of diabetic wound healing [32]. This was based on proteomic characterization of tissue lysates obtained from wound biopsies in patients, whose wound outcome could be defined as rapidly healing (RH, n=17) or non-healing (NH, n=11). Briefly, proteomic analysis was performed with iTRAQ labelling and mass spectrometry on Matrix-Assisted Laser Desorption/Ionization Time-of-Flight (MALDI/TOF) and Orbitrap. After bioinformatic analysis of peptides and sequence coverage, data were filtered retaining only proteins identified by at least two unique peptides and with a false discovery rate <5%. Abundance of individual proteins was expressed as the NH/RH ratio, with confidence interval derived from technical triplicate over the background generated by swapping iTRAQ labels. We herein analyzed data to evaluate whether proteins associated with NETs showed differential abundance in NH versus RH wounds. To this end, we built a custom pathway made up of proteins that have been associated with NETs. A PubMed search was run on Sept 2014 with search string ("NETs" or "neutrophil extracellular traps" or "NETosis"): two reviews of the literature, published in 2013 and 2014 provided the best and updated overview of NET-associated proteins. This list was matched with the list of proteins identified in diabetic wounds as described above. Proteins were divided into groups according to the belonging cellular compartment (nucleus, granules, cytoplasm, cytoskeleton, plasmamembrane). Individual protein relative expression was retrieved, and the average relative expression of each compartment was calculated. To validate the measure of NET-associated proteins in individual wound lysates, we used samples collected from patients of a "validation cohort", who were divided according to the wound outcome at follow-up in those whose ulcer had worsened and in those whose ulcer was stable or healed. We measured tissue elastase content using the Polymorphonuclear Elastase Human ELISA Kit (Abcam).

Results

Proteomic analysis of NETosis biomarkers

Our group previously demonstrated that high glucose and hyperglycemia increase release of NETs and circulating markers of NETosis, respectively. These findings provide a link among neutrophils, inflammation and tissue damage in diabetes [29].

Screening the literature, we identified 25 proteins, belonging to 5 subcellular compartments (nucleus, granules, cytoplasm/cytoskeleton, enzymes, and plasma membrane), and we used them to create a custom NETosis pathway (see Figure 14 A and B). In our lab, we developed a proteomic-based technique for the identification of new candidate biomarkers and therapeutic targets in diabetic wound healing (see also the material and methods section) [32]. We therefore exploited the potential of this approach to assess the involvement of these proteins in the NETosis process. This strategy is based on a proteomic analysis of wound biopsies obtained from patients with DFUs, who were unequivocally categorized as rapidly healing (RH) or non-healing (NH). Several proteins were identified as differentially expressed in RH versus NH diabetic wounds, from a biopsy of the wound margin using tissue digestion, protein extraction, and proteomic analysis. The expression of granular and nuclear NET components was 2.6- and 2.2-fold higher in NH versus RH wounds, respectively ($P < 10^{-6}$ and $P = 0.002$, respectively). Nongranular enzymes were mildly (1.3-fold) but significantly ($P < 10^{-4}$) enriched in NH versus RH wounds, whereas proteins of the cytoplasm, cytoskeleton, and plasma membrane were not significantly different between the two groups (Figure 14 B and C). The custom NETosis pathway was enriched in NH versus RH wounds, according to Gene Set Enrichment Analysis (GSEA) heat map (Figure 14 D).

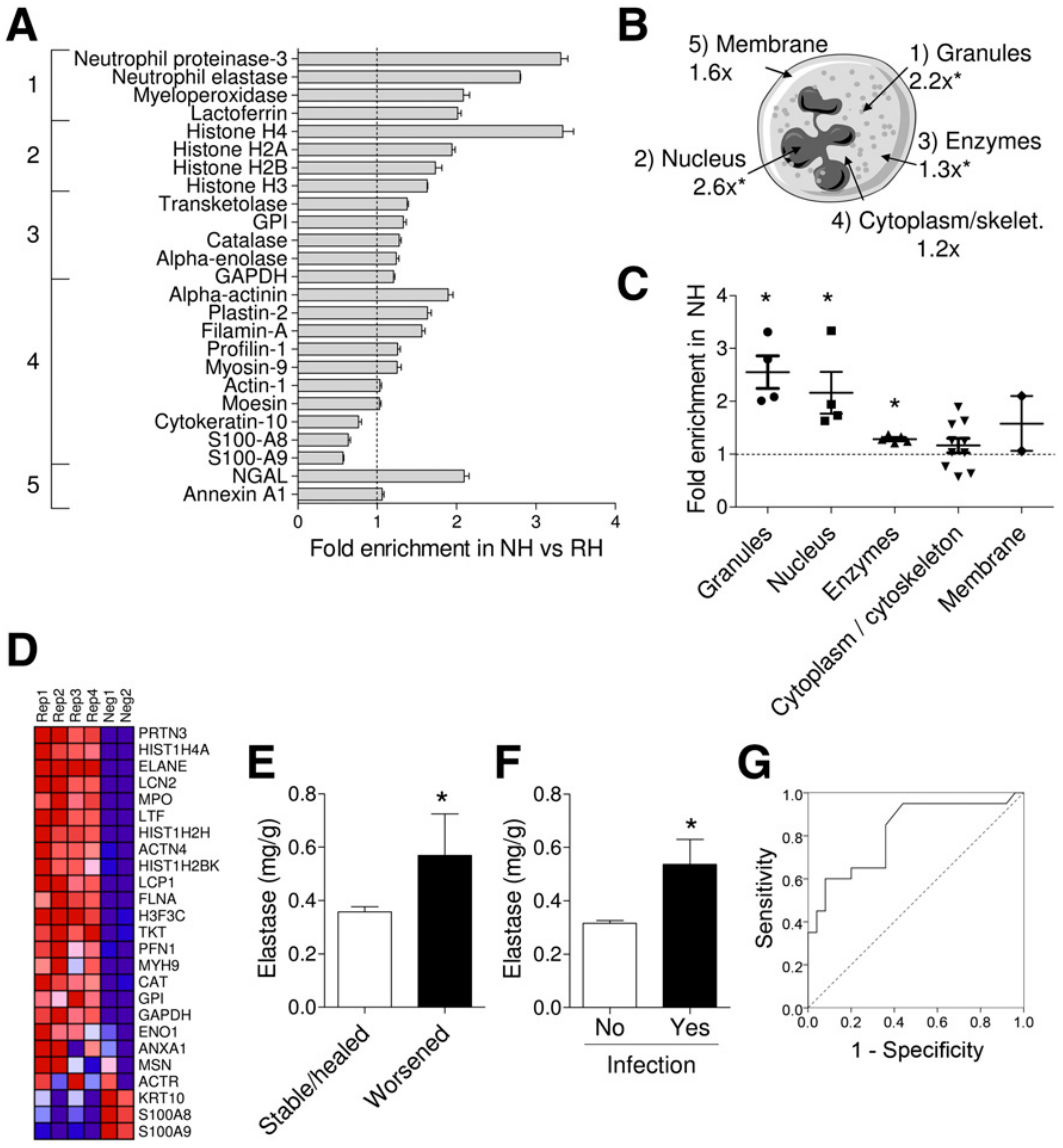

*Figure 14 Proteomic analysis of diabetic wound lysates. (A) Proteins belonging to the custom NETosis pathway are shown with their fold enrichment in NH vs. RH wounds. Error bars were derived from internal technical triplicates of the iTRAQ labels. The dashed line at onefold change aids visual identification of proteins with significant enrichment or depletion in NH vs. RH. Numbers on the left correspond to the cellular compartment illustrated in B. (B) Average fold enrichment for proteins in each subcellular compartment in NH vs. RH of proteins in the custom NETosis pathway (*P < 0.05). (C) Fold enrichment in NH vs. RH with dispersion shown by individual dots of NETosis pathway proteins grouped according to subcellular compartment (*P < 0.05 compared with 1.0). (D) Profile plot from the GSEA showing highly significant enrichment of most proteins of the custom NETosis pathway in the 4 replicates (Rep1–Rep4) compared with negative control subjects (Neg1-Neg2). False discovery rate–adjusted P value for this analysis, according to GSEA output, was <0.001, and normalized enrichment score was 2.06. (E) Wound elastase content (mg elastase/g tissue) in patients of the validation cohort showing stable/healed wounds vs. in those showing worsening wound evolution (*P < 0.05). (F) Wound elastase content in patients of the validation cohort with and without microbiologically proven infection (*P < 0.05). (G) Receiver operating characteristic curve showing the accuracy of wound elastase content in discriminating presence/absence of infection.*

These data indicate that typical granular and nuclear constituents of NETs are increased in the tissue lysates of NH diabetic wounds.

We then quantified NET components (dsDNA, oligo- and mono- nucleosomes, and neutrophil elastase) in the tissue extracts of wound biopsies taken from an independent

validation cohort of patients with DFUs. Patients were divided into two groups based on the wound outcome at a 6-month follow-up: worsening wounds (n = 12) and healed or stabilized wounds (n = 33). Neutrophil elastase, the prototypical NET marker, was 59% higher in worsening wounds compared with wounds that were stable or healed (P = 0.03). These data suggest that local NETosis is associated with impaired wound healing (Figure 14 E). Infected wounds (20 of 45) had a 76% higher elastase content compared with noninfected wounds (P = 0.012; Figure 14 F). Based on the receiver operating characteristic curve, elastase quantification showed a high accuracy or identifying the presence of infection (area under the curve 0.815 [95% CI 0.686–0.944]; Figure 14 G).

Circulating NETosis biomarkers in DFU

Data shown in the previous paragraph suggest that NET-associated biomarkers are locally increased in NH wounds. Thus, we quantified NETosis biomarkers in the bloodstream of patients with DFUs, and compared them with those of diabetic patients without DFUs and healthy subjects as control.

Circulating levels of oligo- and mono- nucleosomes, neutrophil elastase, NGAL, and proteinase-3 were significantly higher in patients with DFU compared with diabetic patients without DFUs and healthy volunteers (Figure 15 A, B, D and E); instead circulating level of cell free dsDNA was not significantly increased in patients with DFUs, and the concentration of lactoferrin was not associated with diabetes or DFU (Figure 15 C and F). More than 50% of patients had a microbial infection, mainly caused by Gram-positive bacteria (mostly *Staphylococcus aureus*). *S. aureus* is known to produce and release DNases, which may explain why dsDNA was not significantly increased in the bloodstream of DFU patients.

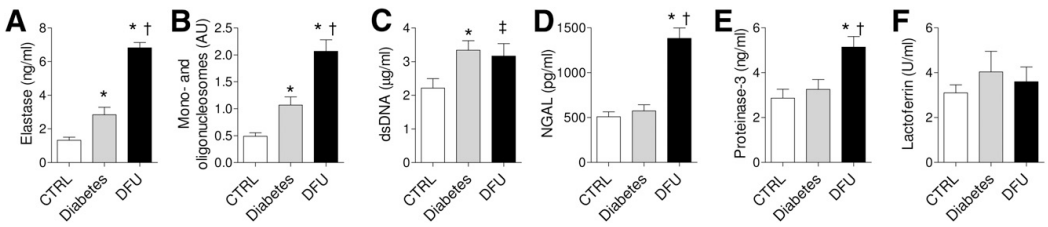

*Figure 15 Circulating NETosis biomarkers in patients with DFU. (A–F) Serum neutrophil elastase (A), mono- and oligonucleosomes (B), cell-free dsDNA (C), NGAL (D), proteinase-3 (E), and lactoferrin (F) concentrations in participants, of which 26 healthy controls (CTRL), 26 diabetic patients without and 52 with DFU (post-ANOVA *P < 0.05 vs. CTRL; †P < 0.05 vs. Diabetes; ‡P = 0.07 vs. CTRL).*

PAD4 is able to promote the citrullination of histones, and in a key enzyme in NETs production. Moreover, it was shown that PAD4 can be released in the extracellular space, to catalyze the citrullination of autoantigen proteins [33]. However, serum PAD4 activity was almost undetectable in all of the patient groups (data not shown). These negative findings indicate that NETosis plays different roles in DFUs and autoimmune disorders.

Patients were followed for an average of 4.5 months. Complete wound healing occurred in 53.8% of patients, partial healing in 17.3% and worsening in 5.7% (minor amputation occurred in 15.4% of patients, major amputation in 9.6% and revascularization in 28.9%). Spontaneous healing without amputation or revascularization occurred in 36.5% of patients.

Figure 16 shows the levels of serum neutrophil elastase in relation to wound outcomes: elastase concentration in patients with completely healed wounds was significantly lower in comparison with patients with NH DFU and it showed a tendency to decrease in patients with spontaneous healing (the latter was defined as complete healing without amputation or revascularization) (Figure 16 A).

A logistic regression analysis showed that serum elastase was significantly inversely associated with complete healing (P = 0.046) after adjustment for infection and ischemia. According to the Kaplan-Meier curves, the probability of spontaneous healing over time was higher in patients with below-median elastase concentrations (P = 0.036) (Figure 16 B).

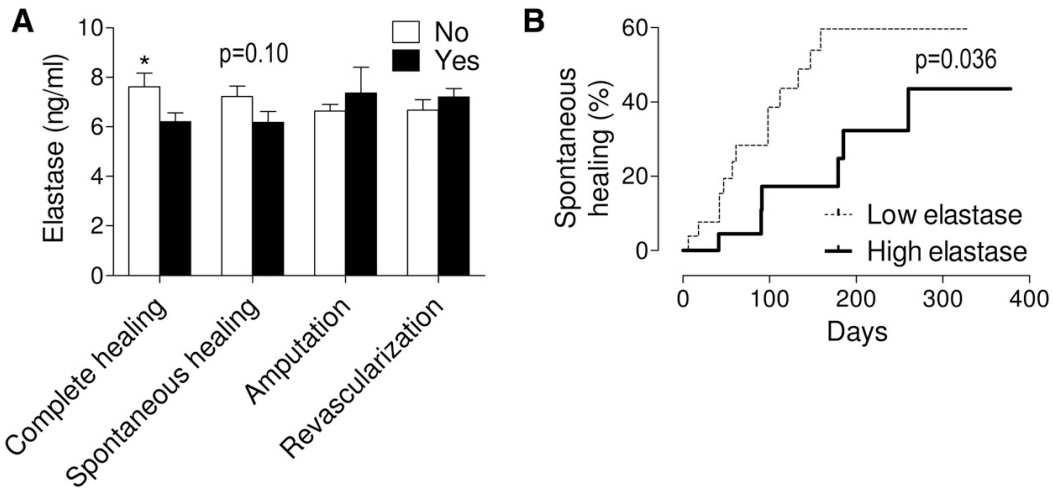

*Figure 16 Circulating elastase and wound outcomes. (A) Serum elastase concentrations are plotted in relation to wound outcomes (*P < 0.05). Minor and major amputations are herein pooled. (B) Kaplan-Meier curves showing the probability of spontaneous healing in patients categorized as having low (below-median) or high (above-median) serum elastase concentrations.*

These data confirmed that DFU patients had elevated circulating NET components.

We next assessed whether the neutrophils isolated from DFU patients were primed toward NETosis. For this purpose, we purified neutrophils using non-activating immunomagnetic cell sorting and then evaluated spontaneous, NOX-dependent, and NOX-independent NETosis by incubating cells with PMA and the Ca^{2+} ionophore a23187, respectively

We estimated NETs release, using quantitative assays for DNA-bound neutrophil elastase and myeloperoxidase (MPO), two NET proteins enriched in diabetic patients with NH wounds. Both elastase and MPO activity assays revealed a significant increase in the number of neutrophils primed for spontaneous NETosis in DFU patients (Figure 17 D-E). The NOX-dependent release of DNA-bound MPO but not elastase was increased in patients with diabetes regardless of DFU (Figure 17 F-G). The NOX-independent release of elastase and MPO in NETs was lower in patients with diabetes compared with control subjects (Figure 17 H-I).

We next calculated the fold induction of NOX-dependent and NOX-independent NETosis compared with the basal NETosis level for each group. There was a defect in NOX-dependent (for MPO) and NOX-independent (for both elastase and MPO) NETosis in patients with DFUs (Figure 17 I-J).

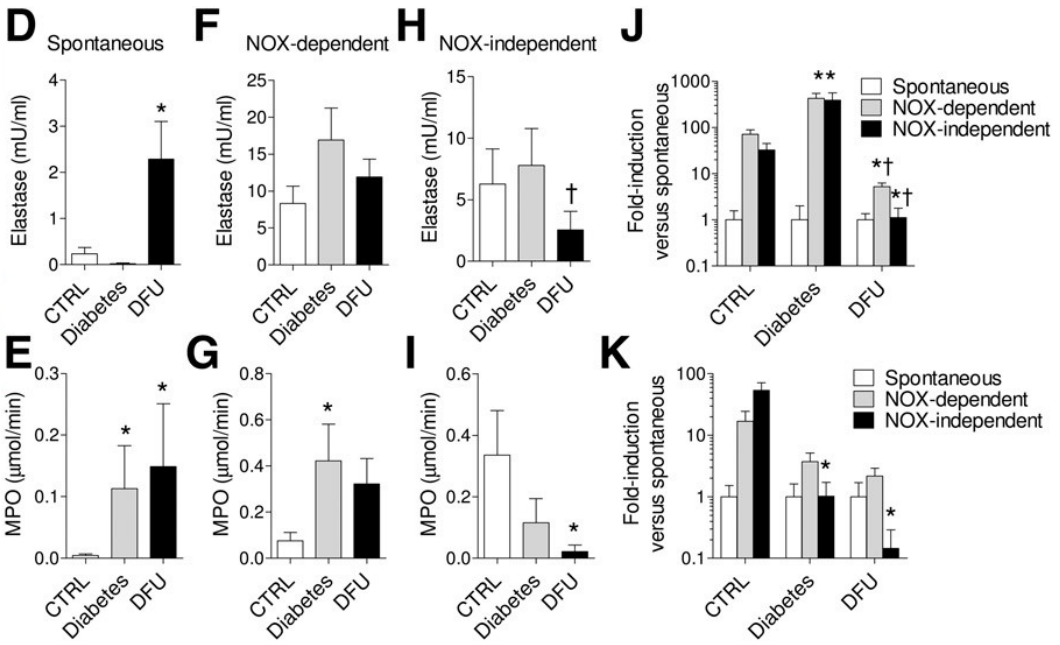

*Figure 17 2—Circulating NETosis biomarkers in patients with DFU. Serum neutrophil elastase (A), mono- and oligonucleosomes (B), cell free dsDNA (C), NGAL (D), proteinase-3 (E), and lactoferrin (F) concentrations in participants without diabetes (CTRL), with diabetes (Diabetes), and with DFU (post-ANOVA *P < 0.05 vs. CTRL; †P < 0.05 vs. Diabetes; ‡P = 0.07 vs. CTRL).*

To summarize, these data suggest that in diabetic patients DFUs prime NETs release. Moreover, the induction of the NETosis process was compromised.

In vitro imaging of NETosis

Next step was to directly visualize single events that take place during NETs release. NETosis was pharmacologically induced in isolated human neutrophils (see below). In first place, we used immunofluorescence labeling of the nucleus, chromatin filaments, and neutrophil elastase. Figure 18 shows the presence of NETs filaments after a 2 h stimulation with PMA.

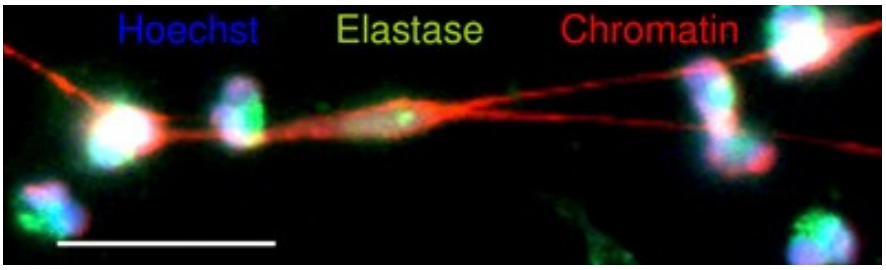

Figure 18 Immunofluorescence of NETting neutrophils, which are stimulated with PMA for 2 h and stained with Hoechst 33342 (in blue) for nuclei, chromatin filaments (in red), and neutrophil elastase (in green). The scale bar is 50 µm.

We observed that a fraction of neutrophils incubated with PMA underwent chromatin decondensation and histone citrullination, by a single-cell morphometric analysis. Figure 19 shows condensed chromatin in blue (Hoechst 33342), and de-condensed chromatin in red, visualized by citrullinated histone H3.

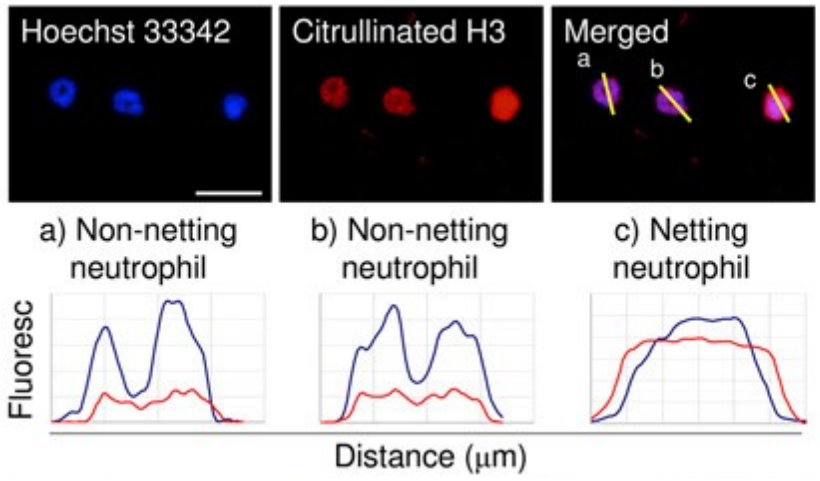

Figure 19 Above, neutrophils stimulated with PMA for 2 h and stained with Hoechst 33342 (blue) and citrullinated histone H3 (red). Below, morphometric analysis of fluorescence signals in neutrophils after PMA-stimulation. The scale bar is 50 µm.

Using transmission electron microscopy (TEM), we confirmed different morphology in NETting neutrophils, which had loss of nuclear lobulation and extrusion of decondensed chromatin compared with unstimulated neutrophils (see Figure 20).

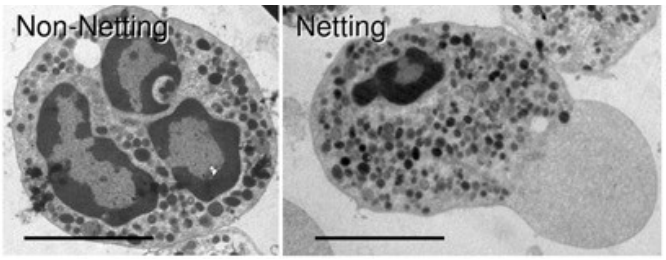

Figure 20 TEM of a non-NETting neutrophil (left) and a NETting neutrophil with loss of nuclear polylobulation (right). The scale bar is 5 µm.

Subsequently, we performed a comparative study on neutrophils using high-resolution live cell imaging to analyze the potential interplay between intracellular calcium, mitochondrial membrane potential, intracellular chromatin decondensation and several morphological features.

We took images up to 2 h using our custom two-photon microscope, and two examples are reported in Figure 21. According to literature [34], we noted that activated neutrophils underwent dramatic morphological changes: the nucleus lost its lobules, the chromatin decondensed, and the inner and outer nuclear membranes progressively detached from each other and, concomitantly, the granules disintegrated. 1 h after activation, the nuclear envelope disaggregated into vesicles and the nucleoplasm and cytoplasm formed a homogenous mass. Finally, the cells rounded up and seemed to contract until the cell membrane ruptured and the interior of the cell was ejected into the extracellular space, forming NETs.

As shown in Figure 21 A, we recorded z-stacks of the same region, at 3 different time points following PMA stimulation:

a) 1 h after stimulation some neutrophils have already undergone NETosis, while others still showed normally energized mitochondria and poly-lobulated nuclei;
b) after 1 h and 20 min, more neutrophils have de-energized mitochondria, with a progressive chromatin decondensation and initial release of NETs (simultaneously stained with Hoechst 33342 and Sytox green);
c) after 1 h and 40 min, extensive release of NETs from many neutrophils was evident.

Figure 21 B contains representative images from a live video recording of the same process, that show a suggestive view of the events taking place during NETosis, from de-energization of mitochondria to delobulation of nuclei and NETs release. The progressive nucleus enlargement and the following NET release, is clearly visible. See also Online Video (https://www.youtube.com/watch?v=2jmwIocwWi0).

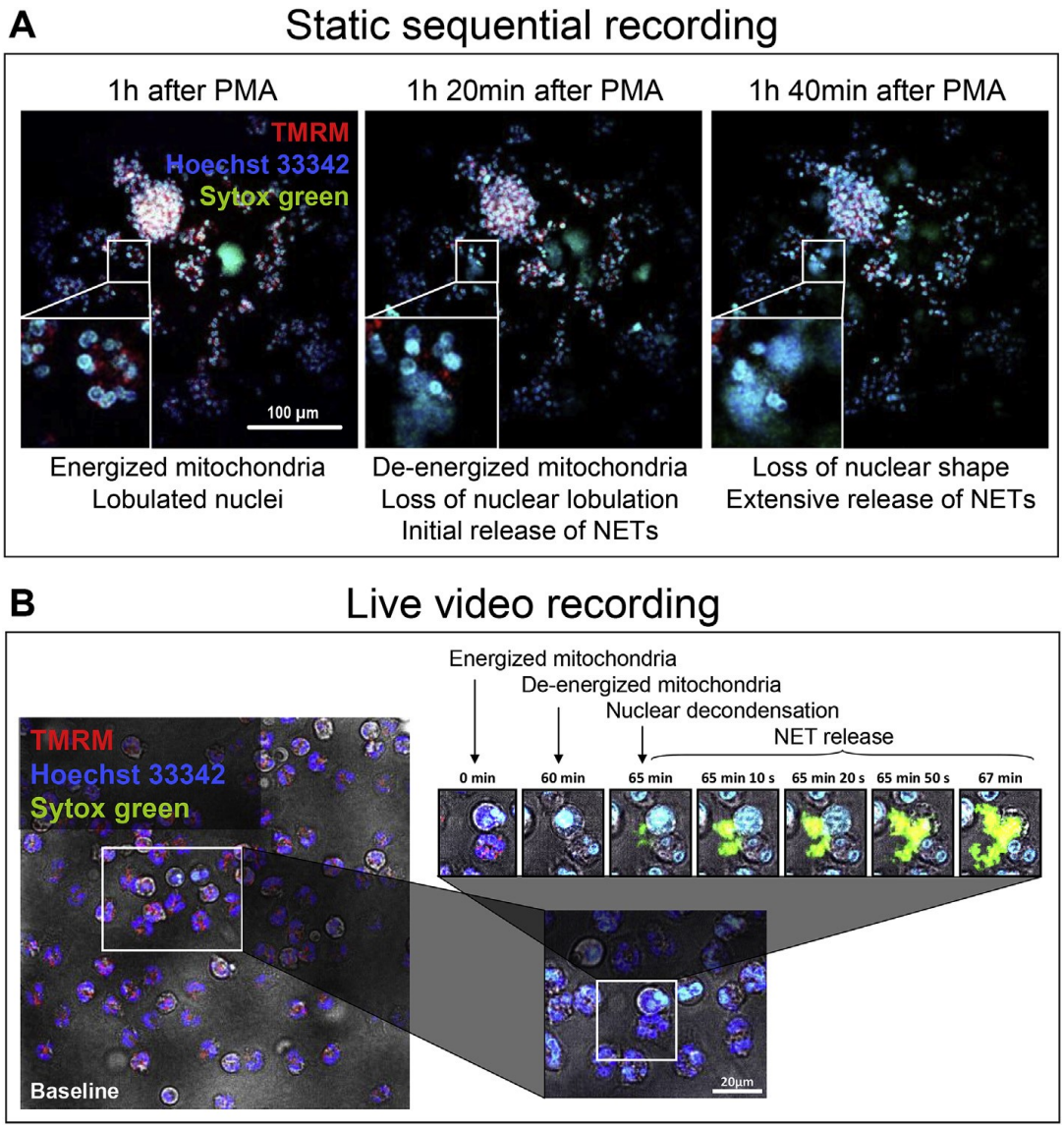

Figure 21 Imaging of NETs formation in vitro. Nuclei are stained in blue with Hoechst 33342; mitochondria are stained in red with TMRM, which labels only energized organelles because its signal is proportional to Δψ; extracellular DNA is stained with Sytox green, present in the medium. Human neutrophils were immuno-magnetically isolated, plated on plastic, stimulated with PMA, and imaged for up to 2h using a custom two-photon microscopy. (A) In these snapshots, it is possible to recognize typical features of the NETosis process. (B) Live recording of the same process allows a suggestive view of the events taking place during NETosis.

NETosis: a typical cell death mechanism

In the previous paragraph, we have illustrated live cell imaging of healthy neutrophils stimulated with PMA, that revealed a cell death program characterized by immediate cell flattening, followed by loss of mitochondrial membrane potential and extrusion of nuclear dsDNA.

We next wanted to establish if the death program induced by PMA was really NETosis, or if other cell death mechanisms are involved, and we did so by stimulating neutrophils in different ways. Neutrophils were either treated with H_20_2 or subjected to UV rays. We noted that neutrophils undergoing apoptosis or necrosis showed phosphatidyl serine (PS) exposure, and indeed their outer cell membrane layer were AnnexinV-positive. In contrast, neutrophils releasing NETs showed membrane rupture and Sytox-positive labelling (Figure 22).

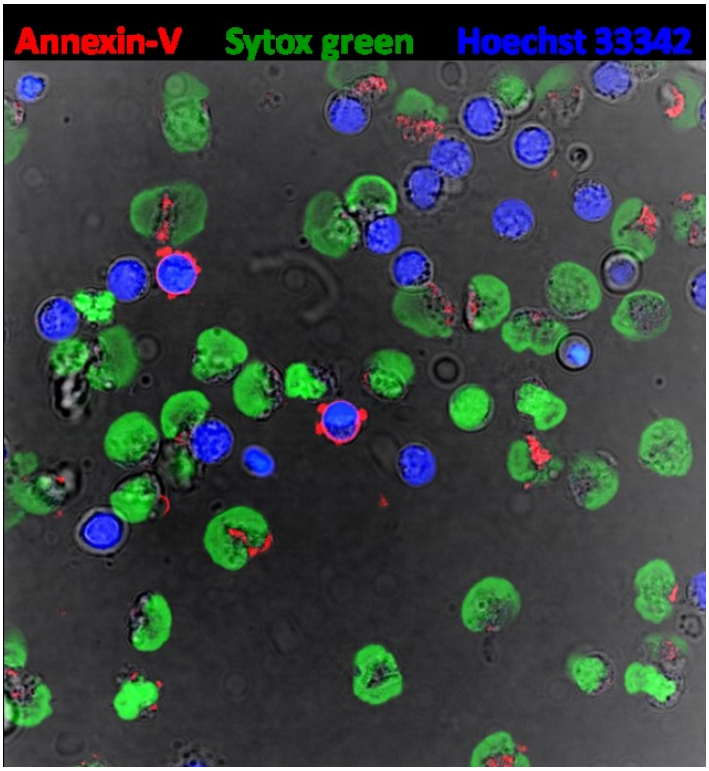

Figure 22 Human neutrophils after 2h of PMA-stimulation: the majority underwent NETosis (Sytox+, green), the remaining were still intact, few went to apoptosis (AnnexinV+, red).

According to Remijsen and colleagues' observations [22], live imaging revealed that H_20_2 did not induce NETosis, as shown by the absence of cell flattening, adherence, massive vacuolization and intracellular chromatin decondensation in intact cells. At 100 µM concentration (well below 8 mM), H_20_2 induced an apoptotic cell death morphology (see Figure 23) whereas, a higher H_20_2 concentration induced a necrotic cell death (data not

shown). These findings demonstrate that H_2O_2-mediated ROS generation is insufficient to induce intracellular chromatin decondensation and subsequent NET formation.

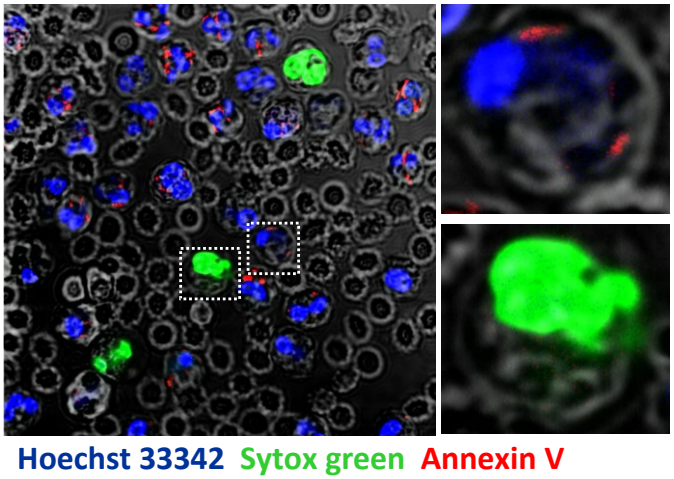

Figure 23 Neutrophils, stimulated with 100 µM H_2O_2, undergone in apoptosis.

We then wanted to study the involvement of caspases in the NETosis cascade. It was reported that NETosis appears as a caspase-independent cell death [17]. We verified this hypothesis by testing how the pan caspase inhibitor affected the kinetics of PMA-induced NETosis. The treatment with 3-[2-(2-benzyloxycarbonylamino-3-methyl-butyrylamino)-propionylamino]-4-oxo-pentanoic acid (z-VAD-FMK) did not affect NETs release kinetics (not shown). Our data are then compatible with the aforementioned hypothesis.

As mentioned, classical necroptosis requires RIP1 (or RIPK1) for the activation of RIP3 through the induction of RIP1/RIP3 necrosomes. However, there have been few RIP3 inhibitors reported yet. B-Raf^{V600E} inhibitors are an important anticancer drug class for metastatic melanoma therapy. Recent study found that B-Raf inhibitors could inhibit RIP3 enzymatic activity *in vitro* [35]. We pre-treated neutrophils with Dabrafenib, which is an inhibitor of the associated enzyme B-Raf, and we noted that it did not affect the kinetics of PMA-induced NETosis (see Figure 24). Our results using Dabrafenib also demonstrate that caspase-independent cell death mediated by RIP1 kinase activity is not implicated in PMA-induced NETosis, which excludes its role in necroptosis.

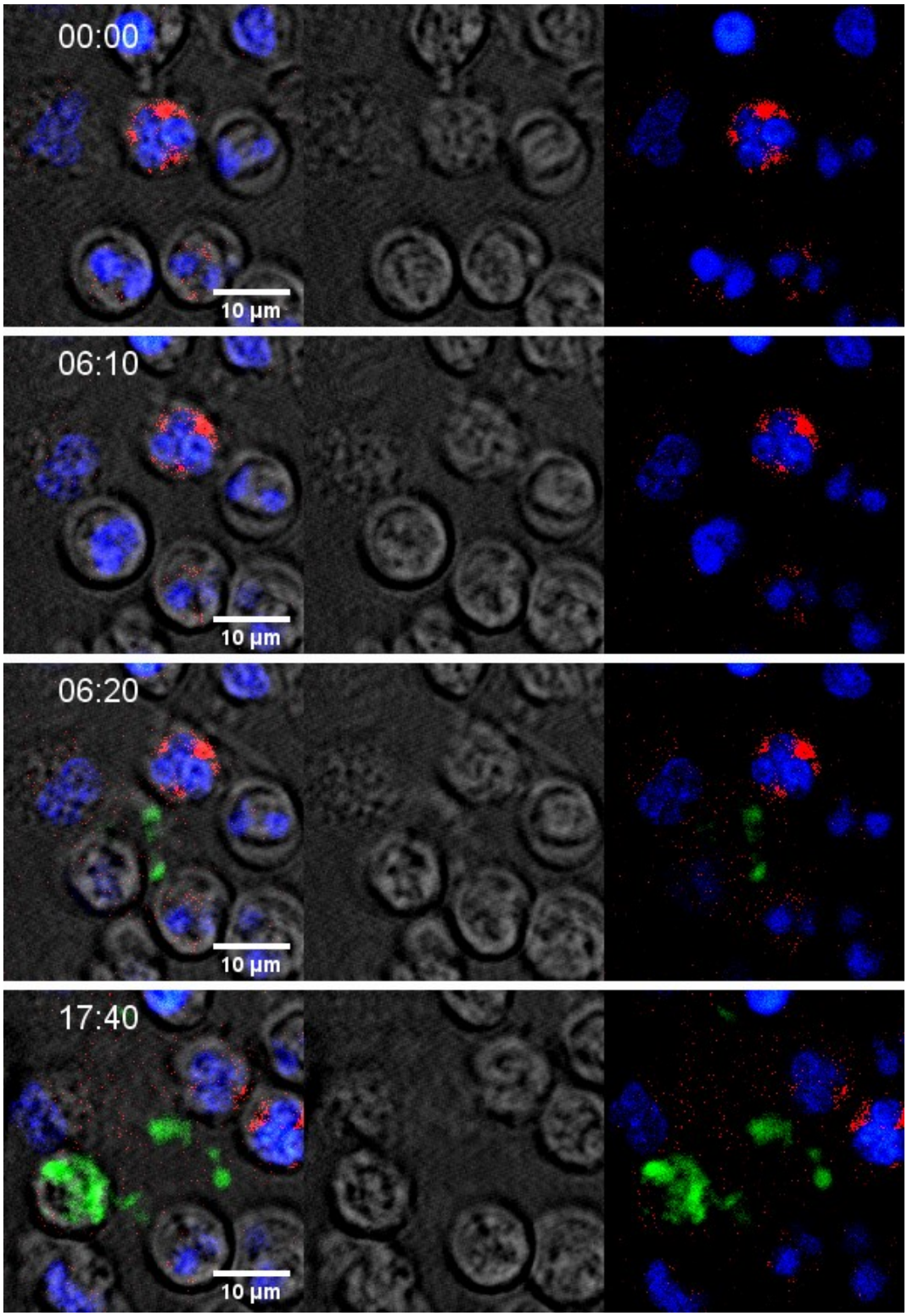

Figure 24 Different time points of neutrophils, stimulated with PMA and treated with Dabrafenib.

All the above experiments confirmed that neither inhibition of caspases by zVAD-fmk nor inhibition of RIP1 kinases by Dabrafenib affected NETosis. Thus, NETosis should be considered a distinct cell death program

Intracellular Ca^{2+} triggers NET release

NETosis has been shown to relay on the generation of ROS by activation of the NAPDH oxidase and histone citrullination by PAD4 activity, both of which are Ca^{2+} dependent events [21]. In order to examine the role of Ca^{2+} in this process, we set up a new imaging protocol: we simultaneously monitored cell morphology, chromatin condensation, mitochondria and intracellular Ca^{2+} (for the latter, we used Fluo-4 that permits to achieve better signal to noise ratio; see Figure 25).

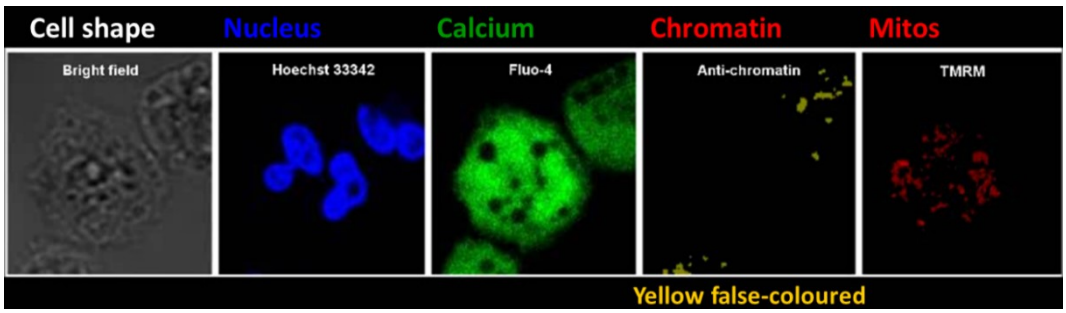

Figure 25 Different channels of visualization of a single human neutrophil, which was pre-loaded with Hoechst 33342, Fluo-4 and TMRM, and anti-chromatin antibody in the medium.

As already reported, NETosis was induced in neutrophils with PMA. We noted that, in parallel with peculiar characteristics of NETosis (changes in cell morphology and chromatin arrangement), intracellular Ca^{2+} had fluctuations. As shown in Figure 26, in the phase preceding the release of NETs, Ca^{2+} signal decreased and we saw a peak in fluorescence intensity, during nuclear DNA decondensation.

See also Online Video (https://youtu.be/8VeEP-GyYYM)

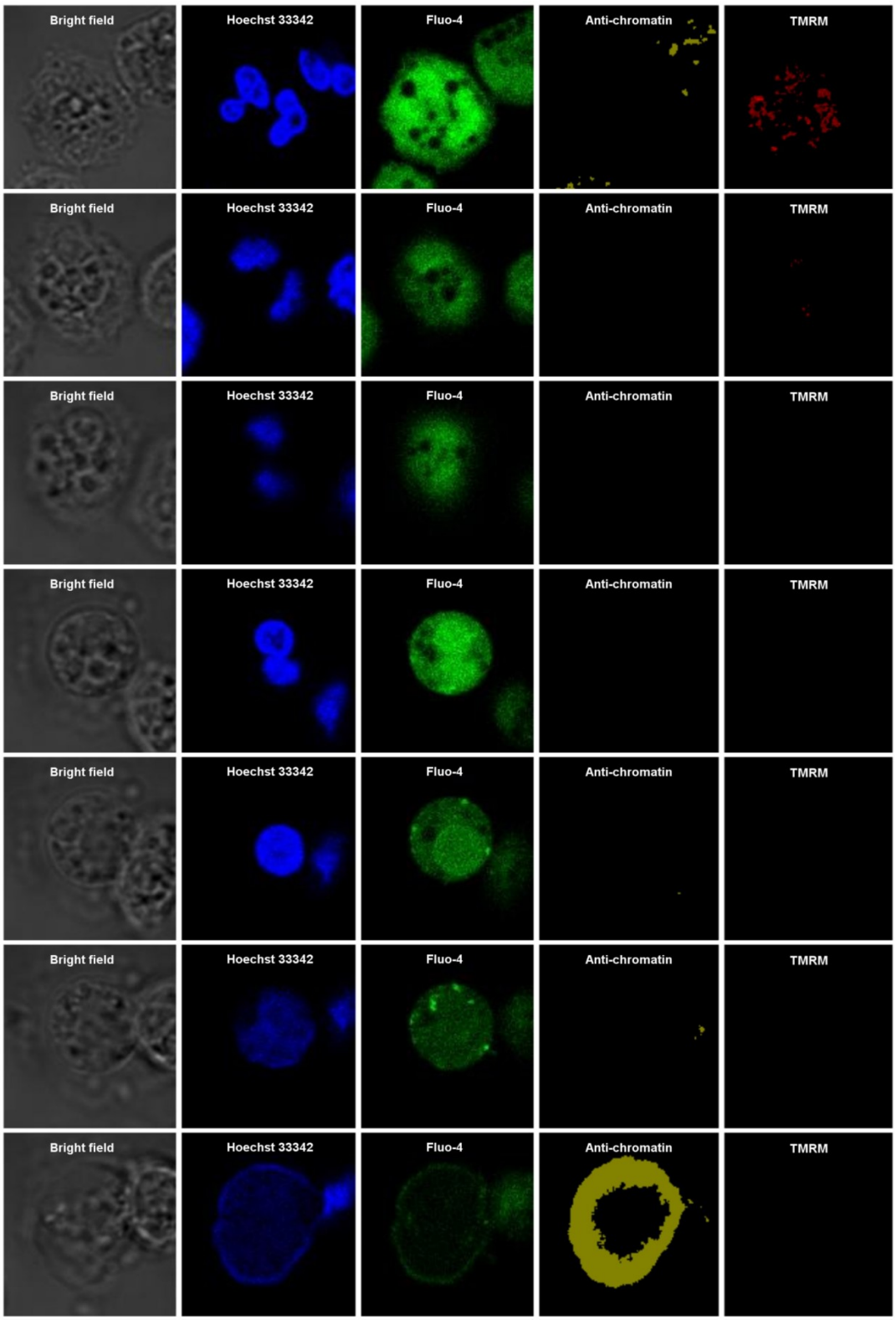

Figure 26 Snapshots of PMA stimulated neutrophil show the simultaneous trend of cell morphology, nuclear DNA, Ca^{2+}, decondensed chromatin and mitochondria potential.

Figure 27 displays the plot of the fluorescence intensity variation over time, of all the channels reported in previous experiment.

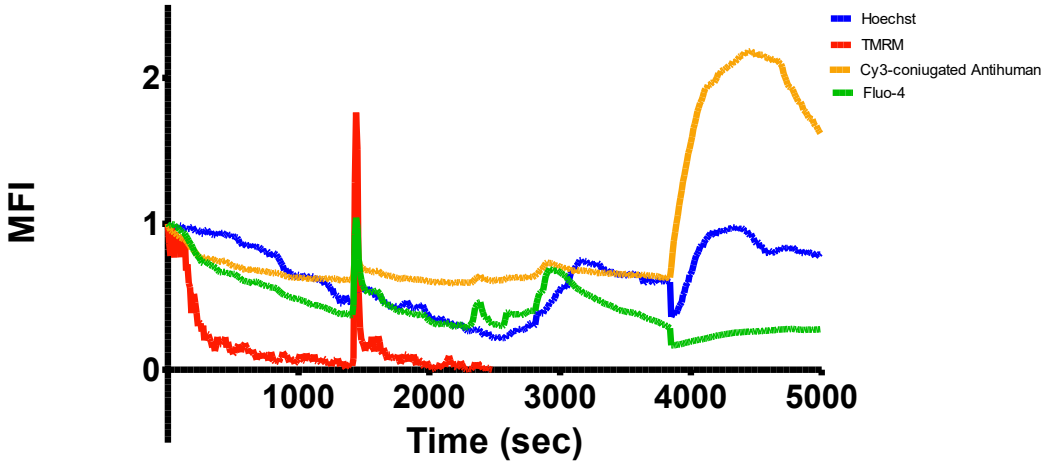

Figure 27 Graph of simultaneous fluorescence signals in stimulated neutrophil: condensed chromatin (blue), energized mitochondria (red), decondensed chromatin (yellow) and intracellular calcium (green).

We, moreover, induced ionomycin stimulus in PMA-treated neutrophils (data not shown).

Thus, our data demonstrate that the induction of NETosis requires mobilization of intracellular calcium pools.

In vivo imaging and FACS analysis in the wound bed

In the previous paragraphs, I showed data regarding the *in vitro* characterization of the NETosis process. We then investigated the role of NETosis in wound healing. As already mentioned, wound healing involves inflammation process and neutrophil recruitment from the nearby tissue. In order to detect *in vivo* neutrophil activation and NETs release, we developed a technique of intravital imaging in an ulcer mouse model.

First, we tried to visualize neutrophils in the intact hind limb skin of mice. Neutrophils were detected only in capillaries (Figure 28).

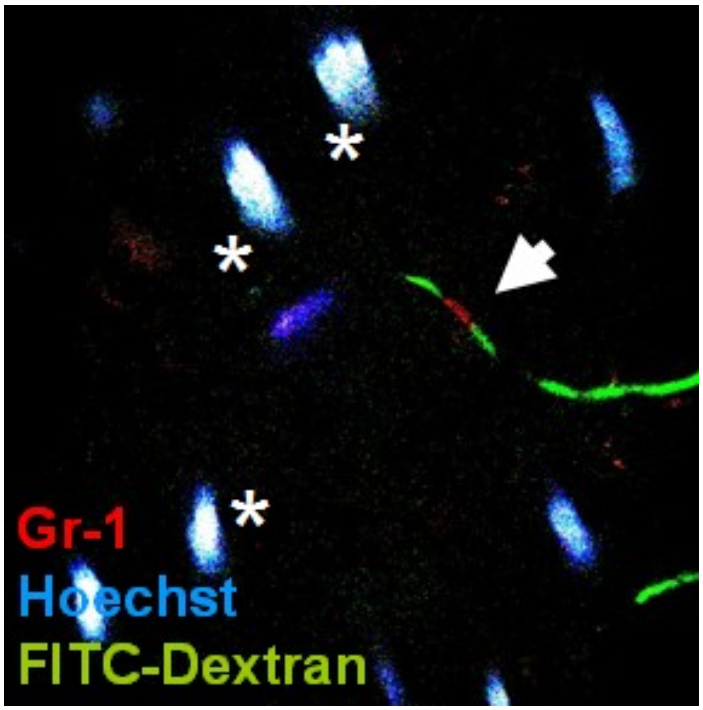

Figure 28 Intravital microscopy imaging of neutrophils and the vasculature in the intact skin. Neutrophils are marked by PE-antiGr-1 (red, arrow), and skin capillaries are stained with high–molecular weight fluorescein isothiocyanate (FITC)–conjugated dextran (green). There is autofluorescence caused by hair bulbs (asterisks).

Next, we experimentally wounded the skin of control non-diabetic mice, and checked them 3 days later. As shown in Figure 29, Gr-1^{+} neutrophils were present at the site of the ulcer, and the majority of them were in NETosis. In Figure 29 A, collagen structures visualization is generated by Second-Harmonic Generation signal (for more details, see SHIM in the "Multiphoton microscopy" chapter). Even though there were motion artifacts, mainly due to heart beat or breathing, we managed to visualize the wound bed at very high magnification. In Figure 29 D, a single neutrophil with decondensed chromatin can be seen in the process of casting NETs, as evidenced by the Sytox green staining in the close vicinity.

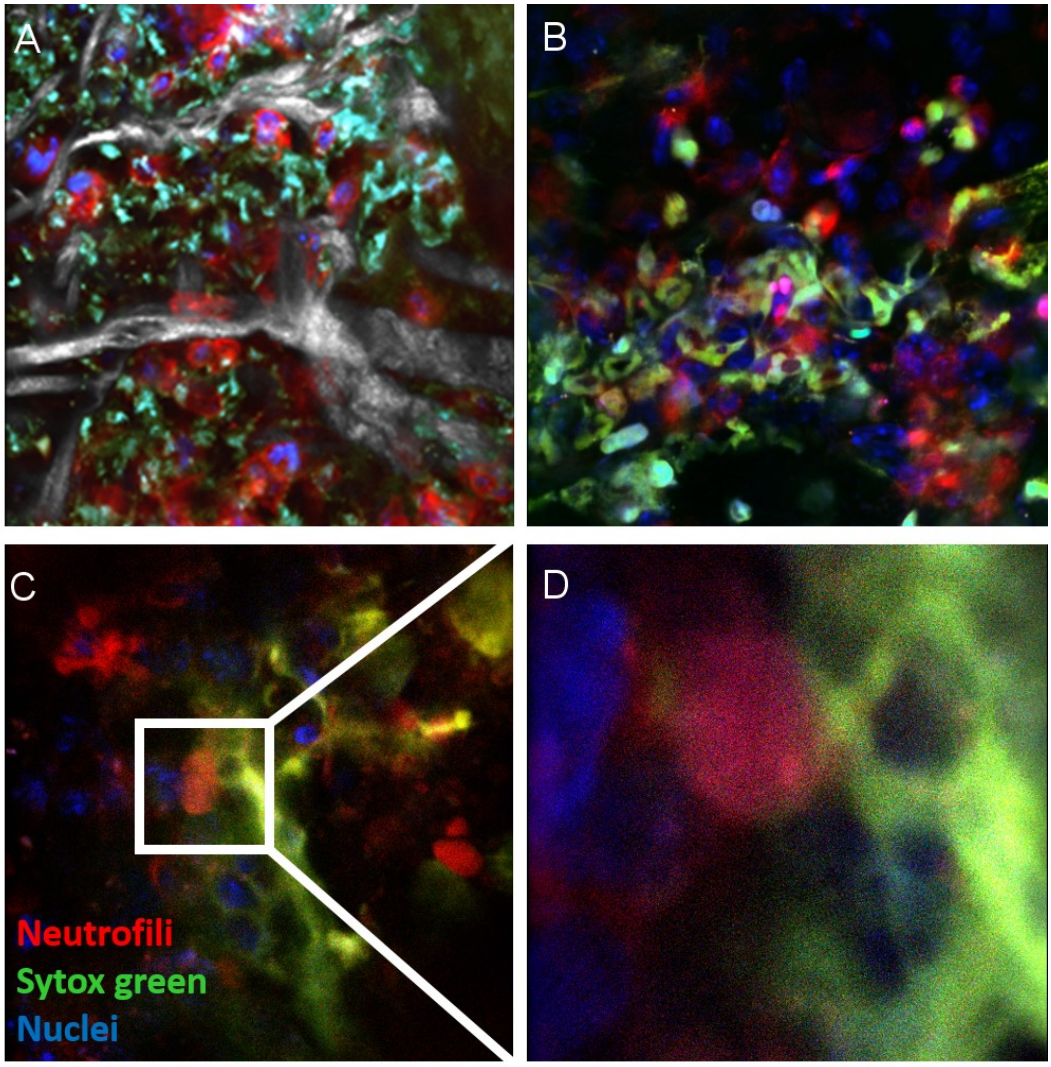

Figure 29 Neutrophils (Gr-1⁺, in red) infiltrated the wound bed. Nuclei are counterstained with cell-permeable Hoechst 33342 (in blue), whereas extracellular cell-free dsDNA (in green) is stained with the cell-impermeable Sytox green dye. Scale bar 50 µm (A, B and C), 5 µm (D).

We then validated imaging data through the analysis of tissue lysates by flow cytometry. Wounded skin contained larger amounts of Gr-1^{+} neutrophils, compared with intact skin. Furthermore, a greater percentage of neutrophils with citrullinated histones H3/4 was found in wounded skin samples, compared with intact skin (Figure 30).

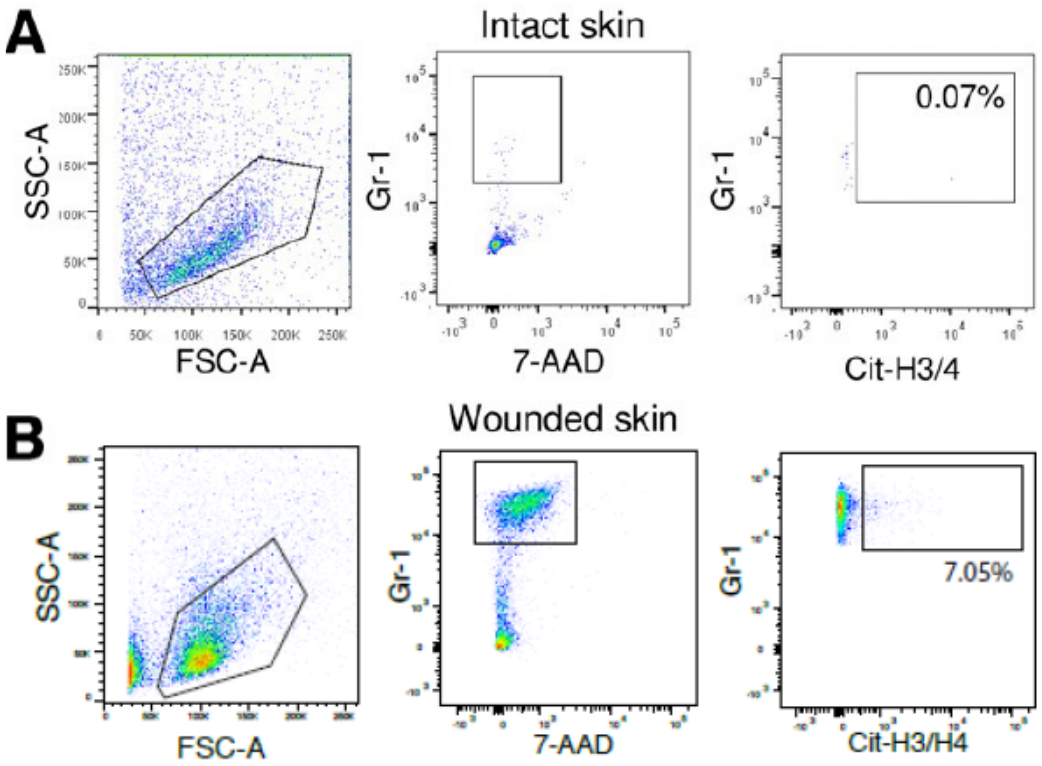

Figure 30 A representative FACS plot showing that Gr-1+ neutrophils are very rare in the tissue lysate of the intact unwounded skin (A) and of wounded skin.

In vitro *treatment with PAD4 inhibitor*

Afterwards, we tested the mechanistic ability of NETosis to delay wound healing. Since NETosis is triggered by PAD4 activation, we used its pharmacological inhibitor Cl-amidine. Neutrophils in which NOX-dependent NETosis was induced by PMA treatment *ex vivo*, were treated with Cl-amidine, and imaged for over 2 hours. As shown in Figure 31, many control cells released DNA, while on the contrary the great majority of the Cl-amidine-treated neutrophils still had lobulated nuclei.

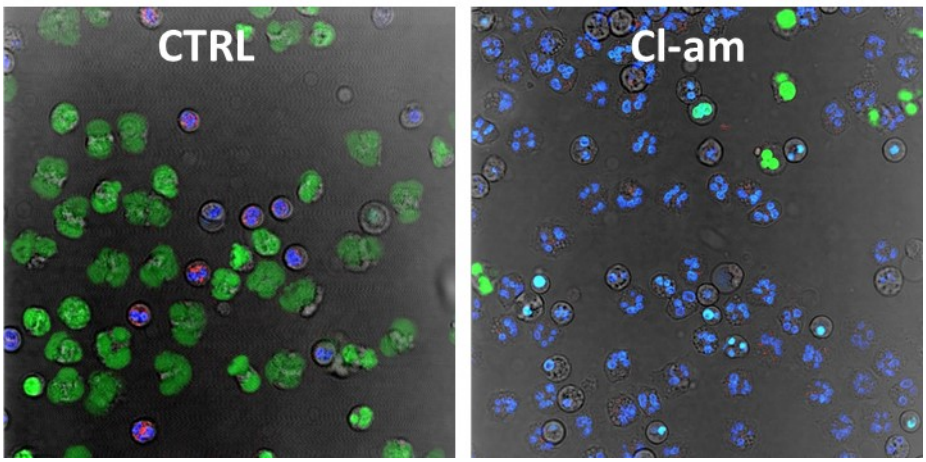

Figure 31 The comparison of neutrophils with or without treatment of Cl-amidine, after 2 h of PMA-stimulation: Sytox⁺ neutrophils were undergone in NETosis.

We also wanted to check the effects of Cl-amidine on the ionomycin-induced NOX-independent NETosis. Figure 32 shows representative FACS analysis for citrullinated histones H3/H4 (Cit-H3/4), indicating that Cl-amidine pretreatment was able to reduce the number of neutrophils undergoing NETosis.

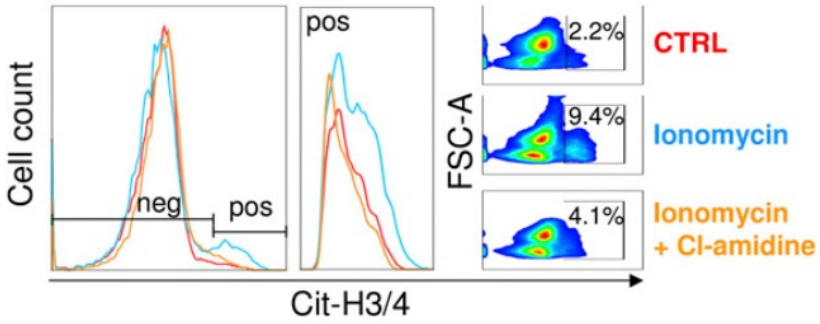

Figure 32 FACS staining for citrullinated histones H3/4 (Cit-H3/4) of mouse neutrophils stimulated with ionomycin with (orange) or without (blue) pretreatment with Cl-amidine with respect to the control condition (red). Magnification of the positive events with mean fluorescence intensity as well as the respective populations and frequencies is shown.

Therefore, we demonstrated that Cl-amidine is able to reduce the induction of NETosis *in vitro*.

Inhibition of NETosis rescue wound healing in diabetic mouse model

The next step was to test the effect of NETosis inhibition in delaying wound healing. To this purpose, we administered Cl-amidine to diabetic mice, in the previously mentioned ulcer experimental model. In these mice, diabetes was induced by a single streptozotocin (STZ) injection (see the "Material and methods" section). PAD4 inhibition was able to reduce the number of neutrophils that underwent NETosis within the ulcer bed, compared with control diabetic mice (Figure 33).

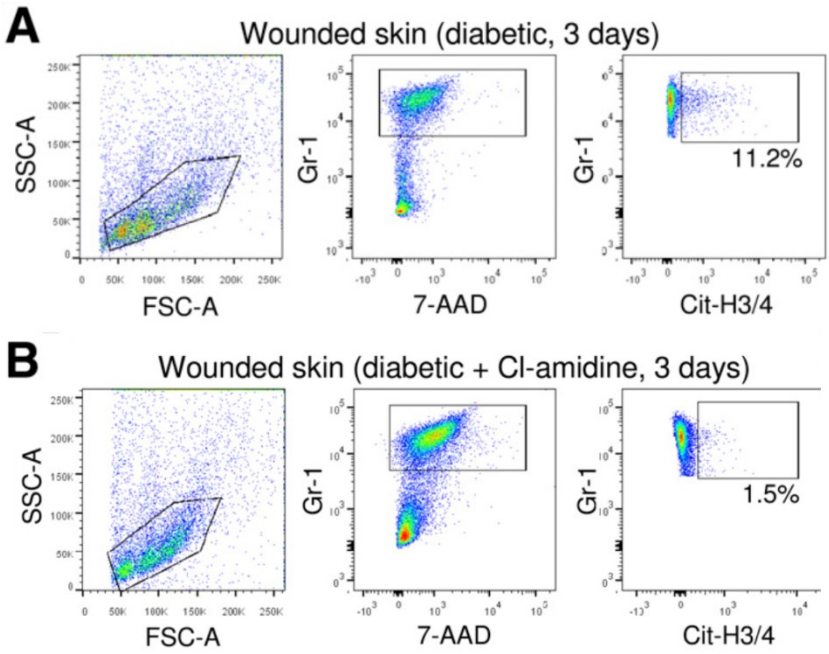

Figure 33 Representative FACS plots showing reduction of citrullinated H3/H4⁺ Gr-1⁺ neutrophils in the skin lysate of diabetic mice treated with Cl-amidine, compared to non-treated animals.

Thus, also the *in vivo* PAD4 inhibition reduced the number of NETting neutrophils, as shown by the decrease in Gr-1$^+$ Cit-H3/4$^+$ cells in the wound of diabetic mice.

We then monitored the effects on NETosis inhibition *in vivo* on wound healing in mice. Figure 34 shows our experimental scheme: mice with STZ-induced diabetes received Cl-amidine treatment or vehicle (DMSO), and the control group non-diabetic mice, which were only injected with vehicle.

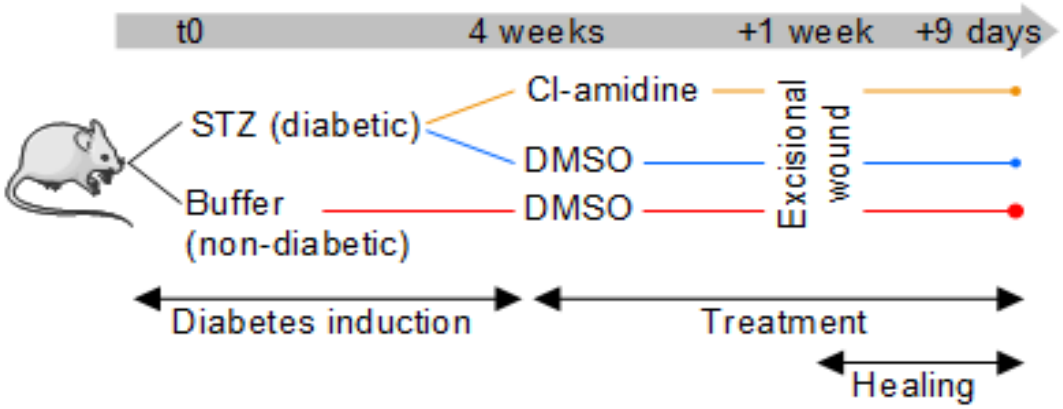

Figure 34 A schematic representation of the wound healing experiment in nondiabetic and streptozotocin (STZ) diabetic with (Cl-amidine) and without (DMSO) pretreatment.

We followed the healing of the ulcers for 10 days: wound healing was delayed in diabetic mice compared with control mice, whereas pretreatment with Cl-amidine restored the normal wound healing in diabetic mice.

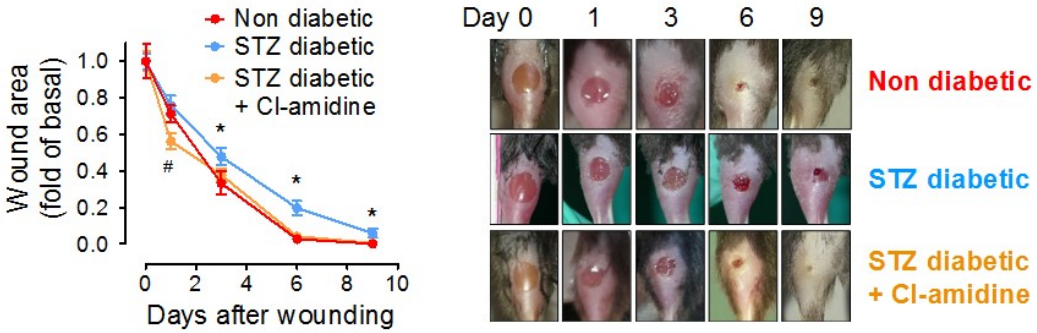

*Figure 35 Wound healing in nondiabetic, STZ diabetic, and diabetic mice treated with Cl-amidine. On the left, the graphic of the fold change in wound area over time (*P < 0.05 for diabetic vs. nondiabetic; #P < 0.05 for Cl-amidine–treated vs. nondiabetic). On the right, a representative digital imaging of wounds from the 3 groups of mice up to day 9.*

Therefore, NETosis inhibition restored the normal healing of diabetic wounds.

Discussion and Conclusions

This work shows for the first time that an excess of NET proteins is associated with impaired wound healing and predicts a poor wound outcome in diabetic patients. In addition, neutrophils isolated from patients with DFU are prone to spontaneous NETosis but shows a defect in inducible NETosis. Two major types of NETosis have been described: (1) NOX-mediated NETosis, activated by PMA [36], and (2) NOX-independent NETosis, which has different signaling requirements [19], typically occurs in response to a S. aureus infection, and can be induced by Ca^{2+} ionophores (for example, ionomycin or a 23187).

NET components, identified in NH wounds using a proteomic analysis (elastase, proteinase-3, NGAL and histones), were found at higher concentrations in the peripheral blood of DFU patients. This systemic NET spreading may be the result of leakage from the wound tissue or production by circulating neutrophils. The latter hypothesis is supported by evidence that neutrophils isolated from the blood of DFU patients are primed for spontaneous NETosis. Therefore, these data identify a systemic component of DFUs that can potentially damage remote tissues and contribute to an overall poor prognosis.

Circulating cell free dsDNA is recognized as a “danger-associated molecular pattern” (DAMP) and can induce an exaggerated activation of innate immunity, whereby inflammation-induced DNA damage and DNA-induced inflammation form a vicious cycle. As a result, NETosis and NET-associated components can induce tissue damage. For instance, NETs have been shown to impair murine aortic endothelium dependent vaso-relaxation and induced endothelial cell apoptosis [37]. On the other side, activated endothelial cells stimulate NETosis and are themselves damaged by NETs. Considering that endothelial dysfunction is considered the *primum movens* of atherosclerosis, it is easy to understand how NETosis can be linked to cardiovascular diseases.

In vitro, we visualized typical NETosis features using immunofluorescence and TEM, but these methods provide variable results [38]. Since NETosis is not well known yet and, moreover, to avoid artifacts derived from fixed samples, we directly visualized in *ex vivo* neutrophils the typical features of NETosis phases. In order to dissect the steps of NETosis, we took advantage of a collaboration with prof. Mammano and Romanato and we deployed a custom two-photon microscope. This imaging setup allowed us to visualize neutrophils at high resolution. We were able to distinguish and characterize *ex*

vivo NETosis process from other cell death programs. Here we described also two major types of NETosis: NADPH-oxidase (NOX) dependent, stimulated by PMA, and NADPH-oxidase independent Ca^{2+}-dependent, induced by Ca^{2+} ionophores. However, the understanding of signaling pathways governing NETs release remains not completely understood.

Moreover, we also used this novel imaging setup for intravital microscopy. Our aim was to detect *in vivo* the NETosis process in the wound bed of our murine model. This method allows for a reliable view of this cell death: *in vivo* imaging is not subject to the biases of fixed-tissue imaging and NETting cells were identified by the typical features, characterized by *in vitro* experiments. This approach is so sensitive that permits the detection of single events of NETs release, within the ulcer.

We cross-validated our live *in vivo* observations through cytofluorimetric analysis. FACS analysis shows that wounded skin contained larger amounts of Gr-1^+ neutrophils, compared with intact skin. Furthermore, a greater percentage of neutrophils with citrullinated histones H3/4 was found in wounded skin samples, compared with intact skin.

Experimental data in mouse indicate that NETosis occurs in the wound bed and may causatively contribute to poor wound healing in diabetic subjects. The increased NETosis and delayed wound healing in diabetes may be due to PAD4. Instead of PAD4 knock-out mice, we pharmacologically inhibited PAD4 activity with Cl-amidine and provided clinically transferrable evidence that NETosis machinery inhibition facilitates wound healing. These findings suggest that NETosis inhibition is a potential therapeutic strategy for wound healing acceleration in DFU patients.

The ability of neutrophils to cast extracellular traps to kill bacteria has been known since more than 10 years, but the role of NETosis in health and disease has been fully recognized only recently. In particular, the involvement of this specific cell death in a multi-organ disease such as diabetes, could lead the way to new therapeutic horizons and new pathophysiological hypotheses. Chronic inflammation is not specific of metabolic disorders, but is also commonly associated with atherosclerosis and cardiovascular disease. Indeed, NETosis is beginning to be explored also in the setting of cardiovascular damage [39]. It has been already mentioned that NETosis and endothelial cell dysfunction can interact to promote vascular damage. Altogether, these recent data on the role played by NETosis in cardiovascular disease are supported by the

observation that systemic levels of putative biomarkers of NETs release associate with the severity of atherosclerosis and predict future cardiovascular events [40]. Besides, an emerging role in atherosclerosis suggests that NETosis may also play a major role in acute myocardial infarction. A double-edged role for this biological process is arising, whereby NETs provide a defense against invasive infections, but can induce tissue injury, thrombosis, impair wound healing and promote cardiovascular disease at the same time. The finely tuned balance required to protect the human body from microorganisms, yet avoiding self-damage, seems to be lost in diabetes. This new perspective on NETosis as a contributor to hyperglycemia-mediated end-organ damage provides for the first time a comprehensive explanation for the tremendous susceptibility of diabetic patients to severe infections and worse infection-related outcomes.

As a future perspective, we are willing to explore the role of NETosis on retinopathy, which is a frequent complication caused by diabetes among the macrovascular and microvascular disorders. The mechanisms leading to the neurodegeneration of the retina in diabetic patients include: low-grade inflammatory process, oxidative stress, activation of polymorphonuclear neutrophils, glutamate excitotoxicity and imbalance in the neuroprotective factors [41]. These aspects suggest a possible role of NETosis also in diabetic retinopathy.

In conclusion, this study in mice and humans strongly expands our knowledge of the role of NETosis in one of the most threatening diabetes complications: DFU. Our data demonstrate that diabetes causes an over-production of PAD4, which triggers the activation of neutrophils, making them, in turn, more prone to enter NETosis. Hence, NETs production is a key factor which delays wound healing in diabetic patients. In summary, PAD4 inhibition and cleavage of NETs by DNase 1 could be novel therapeutic approaches to wound resolution in diabetes.

References

1. Matough, F.A., et al., *The role of oxidative stress and antioxidants in diabetic complications.* Sultan Qaboos Univ Med J, 2012. **12**(1): p. 5-18.

2. Szablewski, L. and A. Sulima, *The structural and functional changes of blood cells and molecular components in diabetes mellitus.* Biol Chem, 2016.

3. Obrebska, A. and J. Kowalski, *[The prognostic value of hyperglycemia, leukocytosis and decreased glomerular filtration rate in acute coronary syndromes--pharmacological protection capabilities].* Pol Merkur Lekarski, 2014. **37**(220): p. 240-3.

4. Rahelic, D., *[7th Edition of Idf Diabetes Atlas--Call for Immediate Action].* Lijec Vjesn, 2016. **138**(1-2): p. 57-8.

5. Morbach, S., et al., *Long-term prognosis of diabetic foot patients and their limbs: amputation and death over the course of a decade.* Diabetes Care, 2012. **35**(10): p. 2021-7.

6. Brem, H. and M. Tomic-Canic, *Cellular and molecular basis of wound healing in diabetes.* J Clin Invest, 2007. **117**(5): p. 1219-22.

7. Gonzalez, A.C., et al., *Wound healing - A literature review.* An Bras Dermatol, 2016. **91**(5): p. 614-620.

8. Medrado, A.R., et al., *Influence of low level laser therapy on wound healing and its biological action upon myofibroblasts.* Lasers Surg Med, 2003. **32**(3): p. 239-44.

9. Martin, P. and S.J. Leibovich, *Inflammatory cells during wound repair: the good, the bad and the ugly.* Trends Cell Biol, 2005. **15**(11): p. 599-607.

10. Brinkmann, V., et al., *Neutrophil extracellular traps kill bacteria.* Science, 2004. **303**(5663): p. 1532-5.

11. Mantovani, A., et al., *Neutrophils in the activation and regulation of innate and adaptive immunity.* Nat Rev Immunol, 2011. **11**(8): p. 519-31.

12. Lahoz-Beneytez, J., et al., *Human neutrophil kinetics: modeling of stable isotope labeling data supports short blood neutrophil half-lives.* Blood, 2016. **127**(26): p. 3431-8.

13. Fuchs, T.A., et al., *Novel cell death program leads to neutrophil extracellular traps.* J Cell Biol, 2007. **176**(2): p. 231-41.

14. Fadini, G.P., et al., *A perspective on NETosis in diabetes and cardiometabolic disorders.* Nutr Metab Cardiovasc Dis, 2016. **26**(1): p. 1-8.

15. Yang, H., et al., *New Insights into Neutrophil Extracellular Traps: Mechanisms of Formation and Role in Inflammation.* Front Immunol, 2016. **7**: p. 302.

16. Abi Abdallah, D.S. and E.Y. Denkers, *Neutrophils cast extracellular traps in response to protozoan parasites.* Front Immunol, 2012. **3**: p. 382.

17. Remijsen, Q., et al., *Dying for a cause: NETosis, mechanisms behind an antimicrobial cell death modality.* Cell Death Differ, 2011. **18**(4): p. 581-8.

18. Nauseef, W.M., et al., *Assembly of the neutrophil respiratory burst oxidase. Protein kinase C promotes cytoskeletal and membrane association of cytosolic oxidase components.* J Biol Chem, 1991. **266**(9): p. 5911-7.

19. Douda, D.N., et al., *SK3 channel and mitochondrial ROS mediate NADPH oxidase-independent NETosis induced by calcium influx.* Proc Natl Acad Sci U S A, 2015. **112**(9): p. 2817-22.

20. Wong, S.L., et al., *Diabetes primes neutrophils to undergo NETosis, which impairs wound healing.* Nat Med, 2015. **21**(7): p. 815-9.

21. Gupta, A.K., et al., *Efficient neutrophil extracellular trap induction requires mobilization of both intracellular and extracellular calcium pools and is modulated by cyclosporine A.* PLoS One, 2014. **9**(5): p. e97088.

22. Remijsen, Q., et al., *Neutrophil extracellular trap cell death requires both autophagy and superoxide generation.* Cell Res, 2011. **21**(2): p. 290-304.

23. Vanden Berghe, T., et al., *Regulated necrosis: the expanding network of non-apoptotic cell death pathways.* Nat Rev Mol Cell Biol, 2014. **15**(2): p. 135-47.

24. Vandenabeele, P., et al., *Molecular mechanisms of necroptosis: an ordered cellular explosion.* Nat Rev Mol Cell Biol, 2010. **11**(10): p. 700-14.

25. Takei, H., et al., *Rapid killing of human neutrophils by the potent activator phorbol 12-myristate 13-acetate (PMA) accompanied by changes different from typical apoptosis or necrosis.* J Leukoc Biol, 1996. **59**(2): p. 229-40.

26. Yipp, B.G. and P. Kubes, *NETosis: how vital is it?* Blood, 2013. **122**(16): p. 2784-94.

27. Joshi, M.B., et al., *Elevated homocysteine levels in type 2 diabetes induce constitutive neutrophil extracellular traps.* Sci Rep, 2016. **6**: p. 36362.

28. Alexandraki, K.I., et al., *Cytokine secretion in long-standing diabetes mellitus type 1 and 2: associations with low-grade systemic inflammation.* J Clin Immunol, 2008. **28**(4): p. 314-21.

29. Menegazzo, L., et al., *NETosis is induced by high glucose and associated with type 2 diabetes.* Acta Diabetol, 2015. **52**(3): p. 497-503.

30. Vladymyrov, M., et al., *Real-time tissue offset correction system for intravital multiphoton microscopy.* J Immunol Methods, 2016. **438**: p. 35-41.

31. Denk, W., J.H. Strickler, and W.W. Webb, *Two-photon laser scanning fluorescence microscopy.* Science, 1990. **248**(4951): p. 73-6.

32. Fadini, G.P., et al., *The molecular signature of impaired diabetic wound healing identifies serpinB3 as a healing biomarker.* Diabetologia, 2014. **57**(9): p. 1947-56.

33. Spengler, J., et al., *Release of Active Peptidyl Arginine Deiminases by Neutrophils Can Explain Production of Extracellular Citrullinated Autoantigens in Rheumatoid Arthritis Synovial Fluid.* Arthritis Rheumatol, 2015. **67**(12): p. 3135-45.

34. Brinkmann, V. and A. Zychlinsky, *Neutrophil extracellular traps: is immunity the second function of chromatin?* J Cell Biol, 2012. **198**(5): p. 773-83.

35. Li, J.X., et al., *The B-Raf(V600E) inhibitor dabrafenib selectively inhibits RIP3 and alleviates acetaminophen-induced liver injury.* Cell Death Dis, 2014. **5**: p. e1278.

36. Parker, H., et al., *Requirements for NADPH oxidase and myeloperoxidase in neutrophil extracellular trap formation differ depending on the stimulus.* J Leukoc Biol, 2012. **92**(4): p. 841-9.

37. Carmona-Rivera, C., et al., *Neutrophil extracellular traps induce endothelial dysfunction in systemic lupus erythematosus through the activation of matrix metalloproteinase-2.* Ann Rheum Dis, 2015. **74**(7): p. 1417-24.

38. Brinkmann, V., et al., *Automatic quantification of in vitro NET formation.* Front Immunol, 2012. **3**: p. 413.

39. Phillipson, M. and P. Kubes, *The neutrophil in vascular inflammation.* Nat Med, 2011. **17**(11): p. 1381-90.

40. Doring, Y., C. Weber, and O. Soehnlein, *Footprints of neutrophil extracellular traps as predictors of cardiovascular risk.* Arterioscler Thromb Vasc Biol, 2013. **33**(8): p. 1735-6.

41. Araszkiewicz, A. and D. Zozulinska-Ziolkiewicz, *Retinal neurodegeneration in the course of diabetes - pathogenesis and clinical perspective.* Curr Neuropharmacol, 2016.